Quantification of cytokine mRNA

Total RNA was extracted from isolated MAIT cells or control T cells using RNeasy spin columns (QIAGEN, Germantown, MD, USA) and reverse transcribed into complementary DNA using Primescript reverse transcriptase (Takara, Ohtsu, Japan). Levels of IFN-γ and IL-17 mRNA were measured by quantitative PCR using an SYBR Premix Ex Taq Kit (Takara) on a LightCycler1.5 (Roche, Basel, Switzerland). Expression levels relative to those of β-actin are presented. The primer pairs used were as follows: IFN-γ forward, 5′-ACAGGGAAGCGAAAAAGGAGTCAG-3′ and IFN-γ reverse, 5′-CATGGGATCTTGCTTAGGTTGG-3′; IL-17 forward, 5′-CCAGGATGCCCAAATTCTGAGGAC-3′ and IL-17 reverse, 5′-CAAGGTGAGGTGGATCGGTTGTAG-3′ and β-actin forward, 5′-CACTCTTCCAGCCTTCCTTCC-3′ and β-actin reverse, 5′-GCGTACAGGTCTTTGCGGATG-3′.

Results

MAIT cells are reduced in the peripheral blood of MS patients and reflect disease activity

Previously, CD161^{high} 3C10 (Vα7.2)-positive cells have been reported to represent MAIT cells in adult human peripheral blood (13, 19, 20). Therefore, we used this definition of MAIT cells to analyze the frequency of MAIT cells in peripheral blood by flow cytometry in HC and MS patients in remission (MS remission) or in relapse (MS relapse). MAIT cells could be identified as a distinct cell population bearing a Vα7.2$^+$CD161^{high} phenotype in all subjects (Supplementary Figure 1A is available at *International Immunology* Online). Representative profiles of a HC and an MS relapse are shown in Fig. 1(A). In HC, the frequency of MAIT cells among total αβT cells was 3.79 ± 0.52% (mean ±SEM). In MS remission, the frequency of MAIT cells was 2.33 ± 0.39%, which was significantly lower than that in HC (Fig. 1B). The frequencies of Vα7.2$^+$CD161^{low} and Vα7.2$^+$CD161$^-$ or Vα7.2$^-$CD161^{high} populations were not different between HC and MS patients, suggesting that the reduced frequency of MAIT cells in MS patients was not simply due to down-modulation of the Vα7.2 TCR or CD161 molecules in MAIT cells in MS patients. In addition to the DN population, within which MAIT cells were first identified, MAIT cells include also CD4, CD8αα and CD8αβ populations (13). Since all the CD4, CD8αβ, CD8αα and the DN MAIT cell sub-populations were reduced in MS patients compared with HC, the decrease in MAIT cell frequency was not attributed to reduction of a certain sub-population of MAIT cells (Fig. 1C). The frequency of total αβT cells among PBMC was not different between HC, MS remission and MS relapse (61.7 ± 4.7, 65.8 ± 1.9 and 67.85 ± 3.2%, respectively).

The decrease in the frequency of MAIT cells was more profound in MS relapse (0.87 ± 0.24%) (Fig. 1B). MS patients who had at least one attack or had been found to have an active lesion by magnetic resonance imaging within 1 year had significantly lower numbers of MAIT cells compared with patients stable for more than a year (Fig. 1D). Furthermore, when MS relapse patients were followed up for 2–3 months after the attack, the frequency of MAIT cells significantly increased along with the clinical recovery

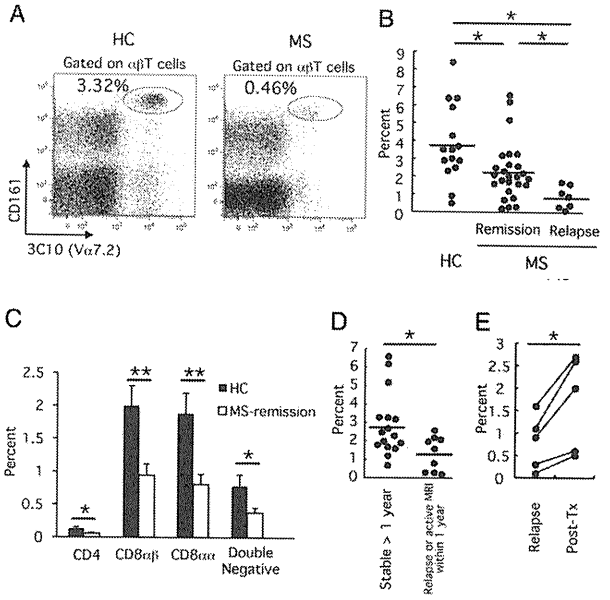

Fig. 1. Frequency of MAIT cells among αβT cells in peripheral blood. (A) Representative flow cytometry profiles of CD3$^+$TCR-γδ$^-$ cells in a HC (left) and in an MS relapse (right). (B) Frequency of MAIT cells among αβT cells in HC (N = 16), MS remission (N = 25) and MS relapse (N = 7). Each symbol represents the value of one individual. Horizontal bars indicate the means. *P < 0.05 (Kruskal–Wallis H-test followed by Mann–Whitney U-test with Bonferroni correction). (C) Frequency of CD4, CD8αβ, CD8αα and DN MAIT cell sub-population among total αβT cells in HC and MS remission. Error bars represent the SEM. *P < 0.05, **P < 0.01 (Mann–Whitney U-test). Since the proportion of MAIT cells in some patients with MS remission and most of those with MS relapse was too low to assess precisely the frequency of each MAIT cell sub-population, they were not included in the analysis. (D) Frequency of MAIT cells in MS patients stable for >1 year and those who had at least one clinical attack or had been found to have active magnetic resonance imaging lesions within 1 year. *P < 0.05 (Mann–Whitney U-test). (E) Frequency of MAIT cells in five patients analyzed at an acute phase of relapse and 2–3 months after steroid therapy (Post-Tx). *P < 0.05 (Wilcoxon t-test).

(Fig. 1E). These results indicate that the frequency of MAIT cells in peripheral blood is reduced in MS remission and reduced even more profoundly in MS relapse, and the frequency reflected disease activity.

The positive correlations in the frequency of MAIT cells with those of CD4$^+$iNKT cells and CD56^{bright} NK cells are lost in MS.

Since several other innate lymphocytes such as CD4$^+$iNKT cells and CD56^{bright} NK cells are believed to participate in the regulation of MS (8, 21), we next examined the correlations of the frequency of MAIT cells with the frequencies of those innate lymphocytes. As shown in Fig. 2 (upper panels), positive correlations between the frequencies of MAIT cells and those of CD4$^+$iNKT cells and CD56^{bright} NK cells were observed in HC. In MS patients, however, the frequency of CD56^{bright} NK cells was decreased along with MAIT cells (Fig. 2, lower right panel). In the case of CD4$^+$iNKT cells, the positive correlation with MAIT cells that was observed in HC was disrupted in MS (Fig. 2, lower left panel).

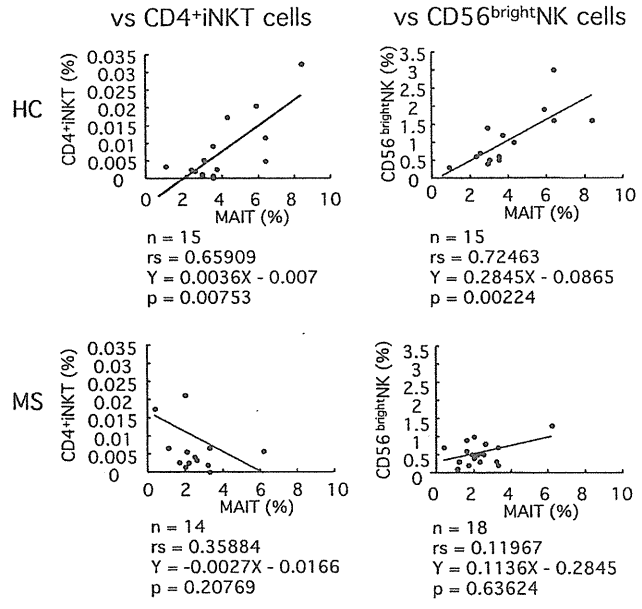

Fig. 2. Correlation of the frequency of MAIT cells with the frequency of $CD4^+$iNKT cells and $CD56^{bright}$ NK cells. The frequency of MAIT cells was plotted against the frequency of $CD4^+$iNKT cells ($CD3^+CD4^+$TCR-$V\alpha24^+$-$V\beta11^+$) among total T cells (left panels) or that of $CD56^{bright}$ NK cells ($CD3^-CD56^{bright}$) among total lymphocytes (right panels) in HC (upper panels) or in MS remission (lower panels). Correlations were analyzed using Spearman's correlation.

Characterization of MAIT cells in HC and MS

To further characterize MAIT cells, we analyzed the expression of chemokine receptors important for CNS invasion. Compared with other T cells, MAIT cells exhibited higher expression of CCR5 and CCR6 (Fig. 3A, top panels), although the expression levels were not different between HC and MS (Fig. 3A, lower panels). We next assessed cytokine production from MAIT cells purified from the PBMC of HC. In response to PMA and IM stimulation, MAIT cells produced substantial levels of IFN-γ and IL-17 (Fig. 3B) but not IL-4 or IL-10 (data not shown). However, none of these responses was observed when MAIT cells were stimulated through CD3 and CD28 (Fig. 3B). These results suggest that the activation of MAIT cells is differently regulated from that of conventional T cells. Intracellular cytokine staining also revealed that MAIT cells produced high levels of IFN-γ in response to PMA and IM (Fig. 3C, upper panels). However, interestingly, the proportion of IFN-γ^+ MAIT cells was not different between HC and MS patients (Fig. 3C, middle left panel). We could also detect intracellular IL-17 in response to PMA and IM, but the frequency was substantially lower compared with the frequency of MAIT cells positive for IFN-γ and was not different between HC and MS patients (Fig. 3C, middle right panel). In contrast to these two cytokines, the frequencies of IL-4^+ and IL-10^+ MAIT cells were lower than those of other T cells positive for these cytokines and were not different between HC and MS patients (Fig. 3C, lower panels).

To evaluate the *in vivo* status of MAIT cells, we next measured cytokine mRNA expression in MAIT cells isolated from HC or MS without additional stimulation. As shown in Fig. 3(D), expression levels of IFN-γ and IL-17 in MAIT cells were not different from control T cells, and the values were comparable between HC and MS patients.

MAIT cells suppress IFN-γ production from T cells in a cell contact-dependent manner

To address the function of MAIT cells in peripheral blood, we evaluated whether depletion of MAIT cells from PBMC might affect cytokine production from T cells. As shown in Fig. 4(A), IFN-γ production in response to PHA stimulation was increased by depletion of MAIT cells from PBMC derived from both HC and MS patients. The enhanced production of IFN-γ by MAIT cell depletion was also observed when PBMC were stimulated through CD3 or CD3 and CD28 (Supplementary Figure 2 is available at *International Immunology* Online). The enhancement of the production was specific to IFN-γ since other cytokines including IL-4, IL-10 and IL-17 were not altered by depletion of MAIT cells from PBMC (Supplementary Figure 3 is available at *International Immunology* Online). These findings suggested that MAIT cells suppress IFN-γ production from T cells in peripheral blood. This IFN-γ suppression by MAIT cells was confirmed by adding purified MAIT cells back into PBMC from which MAIT cells had been depleted (Fig. 4B).

To further elucidate the mechanism of IFN-γ suppression by MAIT cells, we first examined the involvement of suppressive cytokines such as IL-10 and TGF-β by adding their specific mAbs to the culture. MAIT cell-mediated suppression of IFN-γ production was not altered in the presence of these mAbs (Fig. 4C). We next examined whether MAIT cell-mediated IFN-γ production requires cell contact. As shown in Fig. 4(B), the IFN-γ suppression by MAIT cells could not be observed when the cell contact between MAIT cells and other cells was blocked using transwell inserts. Since we previously showed that ICOS/ICOS-L interaction is involved in the suppression of EAE (15), we next examined the effect of anti-ICOS-L mAb in this culture system. The inhibition of IFN-γ production was similar in the presence of anti-ICOS-L mAb compared with that in the presence of control immunoglobulin (Fig. 4C). We next assessed the requirement for B cells in MAIT cell suppression of IFN-γ since we have previously shown that MAIT cell suppression of EAE was dependent on the presence of B cells in this model (15). However, as shown in Fig. 4(D), B-cell depletion had no effect on MAIT cell-dependent suppression of IFN-γ production. These findings indicate that MAIT cell-mediated suppression of IFN-γ production from T cells in peripheral blood required cell contact but not IL-10, TGF-β, ICOS or B cells.

Discussion

In this study, we show that MAIT cells, which comprise a large cell population in human peripheral blood, are reduced in MS patients, especially in those with active disease. Although the precise mechanism of this reduction of MAIT cells in the peripheral blood of MS patients could not be addressed in our present study, the trafficking of MAIT cells from blood into MS lesions is a possible explanation, especially in patients with active disease and those in relapse since we previously showed that MAIT cells invade MS lesions (16). In support of this idea, we found in this

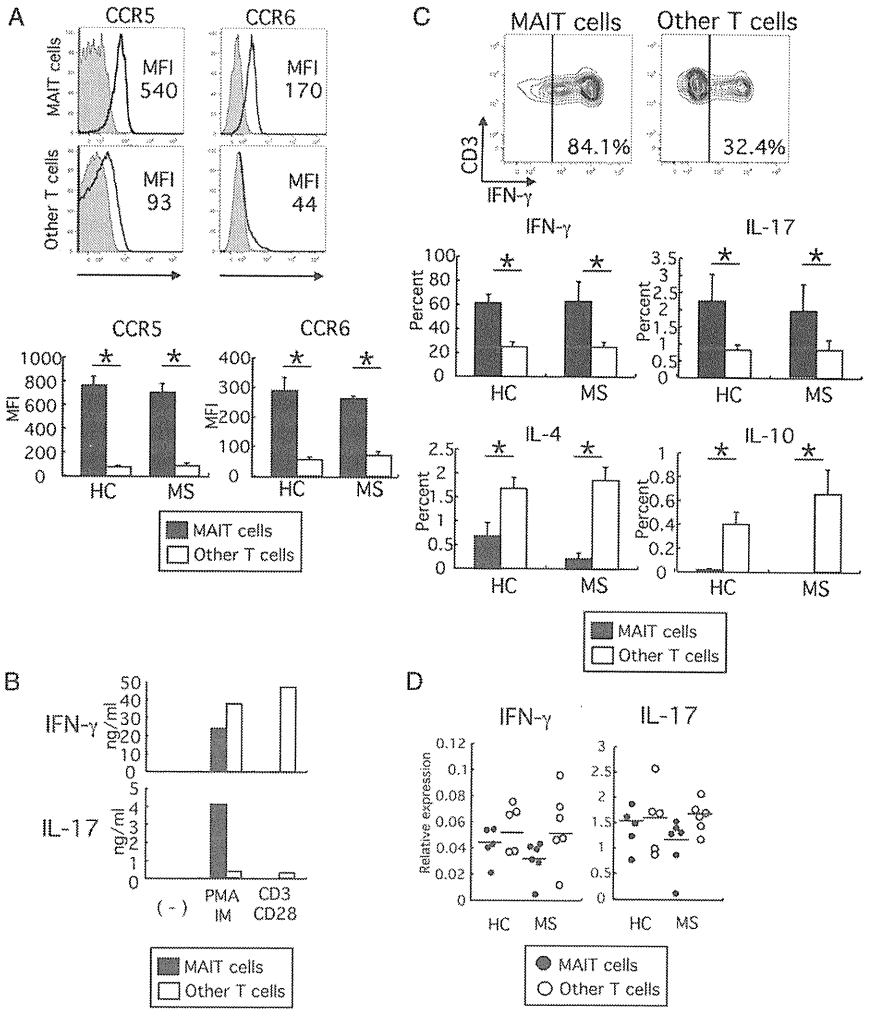

Fig. 3. Phenotype, activation properties and cytokine profile of MAIT cells. (A) Representative histograms of CCR5 and CCR6 expression on MAIT cells ($CD3^+TCR\text{-}\gamma\delta^-CD161^{high}3C10^+$) and other T cells ($CD3^+TCR\text{-}\gamma\delta^-3C10^-$) from an MS remission (upper panels). Bold lines indicate staining of the specific mAb, and shaded histograms indicate background staining of their isotype control antibodies. Mean fluorescence intensity is indicated in each histogram. Results from HC (n = 9) and MS remission (n = 6) are summarized in the lower panels. Error bars represent the SEM. *P < 0.05 (Wilcoxon t-test). (B) IFN-γ (upper panel) and IL-17 (lower panel) production from isolated MAIT cells ($CD5^+CD19^-TCR\text{-}\gamma\delta^-CD161^{high}3C10^+$) and other T cells ($CD5^+CD19^-TCR\text{-}\gamma\delta^-CD161^-3C10^-$) stimulated with PMA and IM or anti-CD3- and -CD28-mAb. Representative results from four independent experiments using cells from three HCs are shown. (C) Intracellular cytokine staining of MAIT cells ($CD3^+TCR\text{-}\gamma\delta^-CD161^{high}3C10^+$) and other T cells ($CD3^+TCR\text{-}\gamma\delta^-3C10^-$). Representative staining profiles of IFN-γ from an MS remission are shown (upper panels), and results of IFN-γ, IL-17, IL-4 and IL-10 staining from HC (n = 8) and MS remission (n = 5) are summarized (lower panels). Error bars represent the SEM. *P < 0.05 (Wilcoxon t-test). (D) IFN-γ (left) and IL-17 (right) mRNA expression in MAIT cells ($CD3^+TCR\text{-}\gamma\delta^-CD161^{high}3C10^+$) and other T cells ($CD3^+TCR\text{-}\gamma\delta^-3C10^-$) isolated from HC ($n$ = 5) and MS remission (n = 6). Each symbol represents the value of one individual. Horizontal bars indicate the means.

study that MAIT cells express high levels of CCR5, CCR6 and α4β1 integrin (data not shown), molecules that are important in the infiltration of T cells into MS lesions, although expression level of these molecules were not different between HC and MS patients. In addition to these findings in MS, it was recently shown that MAIT cells express specific pattern of chemokine receptor (14) and infiltrate lesions resulting from bacterial infection (19, 20), chronic inflammatory demyelinating polyneuropathy (16) and kidney and brain tumors (22). These findings suggest that it is the MAIT cells' character to infiltrate inflammatory lesions.

A second possible explanation for the reduced MAIT cell frequency in the PBMC of MS patients is developmental impairment of MAIT cells in patients. It was previously shown that the development and peripheral expansion of MAIT cells were dependent on the host's microbiological environment (12, 13). In addition, recent epidemiological studies pointed out a universal increase in the prevalence of MS over time (23) and emphasized the importance of changes in environmental factors including sanitation and food quality, factors that affect the profile of intestinal microflora. In this context, our hypothesis is that the change in sanitation status and

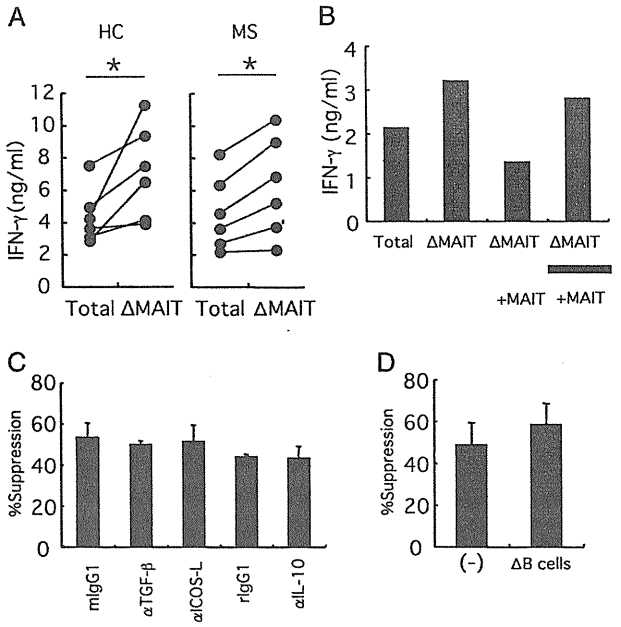

Fig. 4. Suppression of IFN-γ production from T cells by MAIT cells. (A) IFN-γ production from PBMC stimulated with PHA with (ΔMAIT) or without (total) depletion of MAIT cells in HC and MS remission ($n = 6$ each). $^*P < 0.05$ (Wilcoxon *t*-test). (B) IFN-γ production from MAIT cell-depleted PBMC (ΔMAIT) with (+MAIT) or without addition of MAIT cells. Horizontal bar indicates the presence of transwell inserts between MAIT cells and other cells. A representative result from four independent experiments using PBMC from three HCs is shown. (C and D) Efficiency of IFN-γ suppression (%suppression) by MAIT cells in the presence of mAbs against TGF-β, ICOS-L, IL-10 (C) or when B cells were depleted from the culture (ΔB cells) (D). Mean ± SEM of three independent experiments using PBMC from three HCs are shown.

quality of food intake has induced alterations in the profile of gut microflora and impaired the development of MAIT cells and, consequently, resulted in the increased prevalence of MS. On the other hand, genetic factors may also be relevant to an impairment in MAIT cell development in MS. In this regard, it is interesting to note that a single-nucleotide polymorphism in the CD161 molecule, which is expressed at high levels in MAIT cells, has been correlated with MS susceptibility (24); however, the role of this molecule in MAIT cell function and development has not been elucidated.

We observed positive correlations between the frequency of MAIT cells and those of $CD4^+$iNKT and $CD56^{bright}$ NK cells in HC. In contrast, these correlations were not observed in MS patients. These findings suggest the existence of an immune-regulatory link among these innate lymphocyte populations wherein they cooperate to regulate autoimmune responses and imply that the immune pathology of MS is related to a disruption in this regulatory link. In addition, these findings suggest that studies on the immune pathology of MS should not focus only on a single cell population but should also take notice of the system within which the immune cells exist. On the other hand, we cannot deny that these cell populations in peripheral blood are regulated independently. Indeed, while MAIT cells have a propensity to infiltrate inflammatory tissues, $CD56^{bright}$ NK cells are known to migrate into lymph nodes.

An interesting property of human MAIT cells identified in this study is their non-responsiveness to CD3 and CD28 stimulation *in vitro*. This is consistent with a previous report that the $CD8^+CD161^{high}$ T-cell population was not responsive to CD3 and CD28 stimulation even in the presence of exogenous IL-2 (25). We confirmed that most of this $CD8^+CD161^{high}$T cells express Vα7.2 TCR and correspond to MAIT cells. On the other hand, it was recently shown that MAIT cells respond to antigen-presenting cells by producing IFN-γ in an MR1-dependent manner only when the antigen-presenting cells are infected with bacteria (20). These observations suggest a unique activation property of MAIT cells, although the precise mechanism of activation and the cognate antigen are unknown.

We demonstrated in this study that MAIT cells suppress IFN-γ production from T cells and suggest a disease-suppressive role for MAIT cells in MS via suppression of autoreactive T_h1 cells. A suppressive role for MAIT cells was similarly seen in the mouse EAE model and preferential suppression of IFN-γ over other cytokines was also observed in this system (15). With regard to the mechanism of suppression, however, factors other than the requirement for cell contact were quite different between these two species. In mice, the interaction of MAIT cells with B cells through ICOS induced IL-10 production from both cell populations, and this IL-10 up-regulation was associated with EAE amelioration (15). In contrast, we could not detect ICOS expression (data not shown) or IL-10 production by human MAIT cells and suppression of IFN-γ did not require IL-10, ICOS or B cells. In addition, other MAIT cell differences between these species have been reported: human MAIT cells express zinc finger-and BTB domain-containing protein 16 (ZBTB16) transcription factor (26), show a memory phenotype (13, 14), are anergic to CD3 and CD28 stimulation and produce mainly pro-inflammatory cytokines in response to PMA and IM. In contrast, mouse MAIT cells are negative for ZBTB16 (13), show a naive phenotype (13) and respond to TCR stimulation by producing both pro- and anti-inflammatory cytokines (27, 28). The reason for these differences is not clear, but one possibility is the difference in commensal flora that these species are exposed to during their evolution.

In contrast to the present findings, a pro-inflammatory role for MAIT cells in MS cannot formally be ruled out since MAIT cells produced IFN-γ and IL-17 in response to PMA and IM stimulation in this study. Similar finding was reported recently by Dusseaux *et al.* (14). However, similar to us, they could not detect IL-17 production in response to CD3 and CD28 stimulation even in the presence of IL-18 or IL-23, in contrast to the high level of IL-17 and IFN-γ production from MAIT cells stimulated with PMA and IM. Therefore, as the activation properties of MAIT cells are quite unique and as the signal(s) required for MAIT cell activation in MS is largely unknown, conclusions from studies using only PMA and IM do not necessarily reflect the *in vivo* cytokine profile of this cell population. This question requires further studies analyzing the cytokine profile of MAIT cells in MS lesions without exogenous stimulation. In this regard, the results of our cytokine mRNA quantification in unstimulated MAIT cells from peripheral blood are in contradiction to the inflammatory nature of this cell population in MS.

In summary, we show that MAIT cells are reduced in the peripheral blood of MS patients and that their frequency reflects the disease activity of MS. Moreover, we found that MAIT cells, consistent with an immune-regulatory link with other innate immune cell populations, provide a disease-suppressive role in MS by repressing IFN-γ production from T cells. We hypothesize that MAIT cells act as a sensor for environmental changes by responding to alterations in gut microflora by modulating the host's immune system. This property of MAIT cells should be favorable for host defense in most cases but may be disadvantageous in some case including MS. It is possible, however, that a novel treatment for MS might be established by enhancing the immunosuppressive property of MAIT cells through modulation of the host's gut microflora.

Supplementary data

Supplementary data are available at *International Immunology* Online.

Funding

Cabinet Office, Government of Japan (Research Grants on 'Super Special Consortia' for Supporting the Development of Cutting-edge Medical Care to T.Y.); Japan Society for the Promotion of Science (Grants-in-Aid for Scientific Research, S: 18109009 to T.Y., B: 7210 to S.M.); Ministry of Health, Labor, and Welfare of Japan (Research Grants on Psychiatric and Neurological Diseases and Mental Health, 018 to T.Y.) [Health and Labor Sciences Research Grant on Intractable Disease (Neuroimmunological Diseases) to T.Y]; Takeda Science Foundation to S.M.

Acknowledgements

The authors thank Drs Tomoko Okamoto, Norio Chihara and Atsuko Tomita for collection of patient samples and clinical information.

References

1 Sospedra, M. and Martin, R. 2005. Immunology of multiple sclerosis. *Ann. Rev. Immunol.* 23:683.
2 Goverman, J. 2009. Autoimmune T cell responses in the central nervous system. *Nat. Rev. Immunol.* 9:393.
3 Bielekova, B., Goodwin, B., Richert, N. *et al.* 2000. Encephalitigenic potential of the myelin basic protein peptide (amino acids 83-99) in multiple sclerosis: results of a phase II clinical trial with an altered peptide ligand. *Nat. Med.* 6:1167.
4 Miller, D. H., Khan, O. A., Sheremata, W. A. *et al.* 2003. A controlled trial of natalizumab for relapsing multiple sclerosis. *N. Engl. J. Med.* 348:1598.
5 Steinman, L. 2010. Mixed results with modulation of T_H-17 cells in human autoimmune diseases. *Nat. Immunol.* 11:41.
6 Takahashi, K., Miyake, S., Kondo, T. *et al.* 2001. Natural killer type 2 bias in remission of multiple sclerosis. *J. Clin. Invest.* 107:R23.
7 Takahashi, K., Aranami, T., Endoh, M., Miyake, S. and Yamamura, T. 2004. The regulatory role of natural killer cells in multiple sclerosis. *Brain* 127:1917.
8 Araki, M., Kondo, T., Gumperz, J. E., Brenner, M. B., Miyake, S. and Yamamura, T. 2003. Th2 bias of $CD4^+$ NKT cells derived from multiple sclerosis in remission. *Int. Immunol.* 15:279.
9 Viglietta, V., Baecher-Allan, C., Weiner, H. L. and Hafler, D. 2004. Loss of functional suppression by $CD4^+CD25^+$ regulatory T cells in patients with multiple sclerosis. *J. Exp. Med.* 199:971.
10 Porcelli, S., Yockey, C. E., Brenner, M. B. and Balk, S. P. 1993. Analysis of T cell antigen receptor (TCR) expression by human peripheral blood $CD4^-8^-$ α/β T cells demonstrates preferential use of several Vβ genes and an invariant TCR α chain. *J. Exp. Med.* 178:1.
11 Tilloy, F., Treiner, E., Park, S. H. *et al.* 1999. An invariant T cell receptor α chain defines a novel TAP-independent major histocompatibility complex class Ib-restricted α/β T cell subpopulation in mammals. *J. Exp. Med.* 189:1907.
12 Treiner, E., Duban, L., Bahram, S. *et al.* 2001. Selection of evolutionarily conserved mucosal-associated invariant T cells by MR1. *Nature* 422:164.
13 Martin, E., Treiner, E., Duban, L. *et al.* 2009. Stepwise development of MAIT cells in mouse and human. *PLoS Biol.* 7:525.
14 Dusseaux, M., Martin, E., Serriari, N. *et al.* 2011. Human MAIT cells are xenobiotic resistant, tissue-targeted, CD161hi IL-17 secreting T cells. *Blood* 117:1250.
15 Croxford, J. L., Miyake, S., Huang, Y. Y., Shimamura, M. and Yamamura, T. 2006. Invariant Vα19i T cells regulate autoimmune inflammation. *Nat. Immunol.* 7:987.
16 Illés, Z., Shimamura, M., Newcombe, J., Oka, N. and Yamamura, T. 2003. Accumulation of Vα7.2-Jα33 invariant T cells in human autoimmune inflammatory lesions in the nervous system. *Int. Immunol.* 16:223.
17 McDonald, W. I., Compston, A., Edan, G. *et al.* 2001. Recommended diagnostic criteria for multiple sclerosis: guidelines from the international panel on the diagnosis of multiple sclerosis. *Ann. Neurol.* 50:121.
18 Polman, C. H., Reingold, S. C., Edan, G. *et al.* 2005. Diagnostic criteria for multiple sclerosis: 2005 revisions to the "McDonald Criteria". *Ann. Neurol.* 58:840.
19 Gold, M. C., Cerri, S., Smyk-Pearson, S. *et al.* 2010. Human mucosal associated invariant T cells direct bacterially infected cells. *PLoS Biol.* 8:1.
20 Le Bourhis, L., Martin, E., Péguillet, I. *et al.* 2010. Antimicrobial activity of mucosal-associated invariant T cells. *Nat. Immunol.* 11:701.
21 Bielekova, B., Catalfamo, M., Reichert-Scrivner, S. *et al.* 2006. Regulatory $CD56^{bright}$ natural killer cells mediate immunomodulatory effects of IL-2Rα-targeted therapy (daclizumab) in multiple sclerosis. *Proc. Natl Acad. Sci. USA* 103:5941.
22 Peterfalvi, A., Gomori, E., Mafyarlaki, T. *et al.* 2008. Invariant Vα7.2-Jα33 TCR is expressed in human kidney and brain tumors indicating infiltration by mucosal-associated invariant T (MAIT) cells. *Int. Immunol.* 20:1517.
23 Koch-Henriksen, N. and Sørensen, P. S. 2010. The changing demographic pattern of multiple sclerosis epidemiology. *Lancet Neurol.* 9:520.
24 Hafler, D. A., Compston, A., Sawcer, S. *et al.* 2007. Risk alleles for multiple sclerosis identified by a genomewide study. *N. Engl. J. Med.* 357:851.
25 Takahashi, T., Dejbakhsh-Jones, S. and Strober, S. 2006. Expression of CD161 (NKR-P1A) defines subsets of human CD4 and CD8 T cells with different functional activities. *J. Immunol.* 176:211.
26 Savage, A. K., Constantinides, M. G., Han, J. *et al.* 2008. The transcription factor PLZF directs the effector program of the NKT cell lineage. *Immunity* 29:391.
27 Kawachi, I., Maldonado, J., Strader, C. and Gilfillan, S. 2006. MR1-restricted Vα19*i* mucosal-associated invariant T cells are innate T cells in the gut lamina propria that provide a rapid and diverse cytokine response. *J. Immunol.* 176:1618.
28 Shimamura, M., Huang, Y. Y., Migishima, R., Yokoyama, M., Saitoh, T. and Yamamura, T. 2008. Localization of $NK1.1^+$ invariant Vα19 TCR^+ cells in the liver with potential to promptly respond to TCR stimulation. *Immunol. Let.* 121:38.

THE JOURNAL OF BIOLOGICAL CHEMISTRY VOL. 286, NO. 50, pp. 43465–43474, December 16, 2011

GRAIL (Gene Related to Anergy in Lymphocytes) Regulates Cytoskeletal Reorganization through Ubiquitination and Degradation of Arp2/3 Subunit 5 and Coronin 1A*[S]

Received for publication, January 19, 2011, and in revised form, October 5, 2011 Published, JBC Papers in Press, October 20, 2011, DOI 10.1074/jbc.M111.222711

Daiju Ichikawa, Miho Mizuno, Takashi Yamamura, and Sachiko Miyake[1]

From the Department of Immunology, National Institute of Neuroscience, National Center of Neurology and Psychiatry, 4-1-1 Ogawahigashi, Kodaira, Tokyo 187-8502, Japan

Anergy is an important mechanism for the maintenance of peripheral tolerance and avoidance of autoimmunity. The up-regulation of E3 ubiqitin ligases, including GRAIL (gene related to anergy in lymphocytes), is a key event in the induction and preservation of anergy in T cells. However, the mechanisms of GRAIL-mediated anergy induction are still not completely understood. We examined which proteins serve as substrates for GRAIL in anergic T cells. Arp2/3-5 (actin-related protein 2/3 subunit 5) and coronin 1A were polyubiquitinated by GRAIL via Lys-48 and Lys-63 linkages. In anergic T cells and GRAIL-over-expressed T cells, the expression of Arp2/3-5 and coronin 1A was reduced. Furthermore, we demonstrated that GRAIL impaired lamellipodium formation and reduced the accumulation of F-actin at the immunological synapse. GRAIL functions via the ubiquitination and degradation of actin cytoskeleton-associated proteins, in particular Arp2/3-5 and coronin 1A. These data reveal that GRAIL regulates proteins involved in the actin cytoskeletal organization, thereby maintaining the unresponsive state of anergic T cells.

The regulation of T cell activation ensures efficient elimination of pathogens, as well as the maintenance of tolerance to self. Peripheral tolerance prevents the expansion of self-reactive T cells that escaped thymic selection, thus avoiding autoimmunity. T cell anergy is one form of peripheral tolerance that results in nonresponsiveness to antigen rechallenge following an initial partial activation; partial initial activation may result from the stimulation of T cell receptor (TCR)[2] in the absence of co-stimulation or the stimulation of T cells with the calcium ionophore ionomycin (1, 2). The induction of T cell anergy is inhibited by the addition of cyclohexamide, suggesting that anergy induction requires new protein synthesis (3). Recent reports have demonstrated that the induction of E3 ubiquitin ligases, including CBL-b, Itch, Deltex-1, and GRAIL (gene related to anergy in lymphocytes), is required to induce and maintain T cell anergy (4–8). In particular, it is well known that Cbl and Cbl-b act as negative regulators of TCR or CD28 signal transduction cascade through their ability to ubiquitinate tyrosine kinases including Src family kinases such as Fyn and Lck; Syk family kinases such as ZAP-70, Syk, PKC-θ, phospholipase C-γ, and p85; and the regulatory subunit of PI3K (4, 5, 9–15).

GRAIL is a type I transmembrane E3 ligase identified as an early gene that promotes T cell anergy (8). The up-regulation of GRAIL was observed in anergic CD4 T cells after treatment with ionomycin *in vitro* (4). Overexpression of GRAIL in T cell hybridomas or in primary cells reduces IL-2 production as well as proliferation upon antigen stimulation. Naive T cells from *GRAIL*-deficient mice exhibit increased proliferation and cytokine expression upon activation compared with those from control mice and do not depend on co-stimulation for effector generation (16, 17). Moreover, *GRAIL*-deficient mice exhibit lymphocyte infiltration into the lung and kidney and exacerbation of experimental autoimmune encephalomyelitis, indicating an important role for GRAIL in preventing lymphoproliferative and autoimmune responses (17). Although several candidates for GRAIL targets have been reported, including membrane proteins such as CD40 ligand and cytosolic proteins such as Rho GDIs, the mechanisms of GRAIL-mediated anergy induction are still not completely understood (18–21).

T cell activation and function require a structured engagement of antigen-presenting cells. These cell contacts are characterized by prolonged contacts from stable junctions called immunological synapses (IS). Reorganization of the actin cytoskeleton plays an important role in IS formation and signaling. Treatment of T cells with the actin-destabilizing agent cytochalasin D inhibits TCR-mediated IL-2 gene transcription (22). The Arp2/3 (actin-related protein 2/3) complex has been reported to be essential for TCR-mediated cytoskeletal reorganization (23, 24), and Arp2/3 complex-mediated actin nucleation is required for the formation of an F-actin-rich lamellipod (22, 25, 26). Coronin 1A is preferentially expressed in hematopoietic cells and co-localizes with F-actin-rich membranes in activated T cells (27). Coronin 1A has been shown to bind the Arp2/3 complex and inhibit F-actin nucleation by freezing the Arp2/3 complex in its inactive conformation (28). *Coronin 1A*-deficient T cells exhibit reduced cytokine production, including of IL-2 and IFN-γ, and altered F-actin reorganization (29). Moreover, a nonsense mutation in coronin 1A was identified as a gene alteration associated with the Lmb3 locus, which

* This work was supported by Grant-in-Aid for Scientific Research B: 7210 (to S. M.) and Grant-in-Aid for Young Scientists B: 20790093 (to D. I.) from the Japan Society for the Promotion of Science, and Health and Labor Sciences Research Grants for Research on Intractable Diseases from the Ministry of Health, Labor and Welfare of Japan.

[S] The on-line version of this article (available at http://www.jbc.org) contains supplemental text, Table S1, and Figs. S1 and S2.

[1] To whom correspondence should be addressed: 4-1-1 Ogawahigashi, Kodaira, Tokyo 187-8502, Japan. Tel.: 81-423-41-2711; Fax: 81-42-346-1753; E-mail: miyake@ncnp.go.jp.

[2] The abbreviations used are: TCR, T cell receptor; IS, immunological synapse(s); OVA, ovalbumin; Ab, antibody; Ub, ubiquitin.

plays a major role in modulating autoimmunity in Fas^{lpr} mice (30).

In the present study, we demonstrate that both Arp2/3 subunit 5 (Arp2/3-5), a component of the Arp2/3 complex, and coronin 1A serve as substrates for GRAIL. The expression of Arp2/3-5 and coronin 1A is reduced in anergic T cells and in T cells in which GRAIL is overexpressed. Retroviral-driven expression of Arp2/3-5 or coronin 1A in anergic ovalbumin (OVA)-specific T cells restores their proliferation upon antigen activation. The accumulation of F-actin, Arp2/3-5, and coronin 1A at the IS is decreased in anergic T cells as well as in T cells overexpressing GRAIL. Thus, our findings demonstrate that GRAIL maintains the anergic states of T cells by regulating IS formation via degradation of the actin cytoskeleton-associated proteins Arp2/3-5 and coronin 1A.

EXPERIMENTAL PROCEDURES

Reagents and Antibodies—We obtained ionomycin, polybrene, and OVA from Sigma-Aldrich, OVA peptide ($OVA_{323-339}$) from TORAY Laboratory (Tokyo), lactacystin from Boston Biochem Inc., and recombinant IL-2 from Pepro Tech. We purchased antibodies (Abs) against Arp2/3-5 (C3), c-Myc (9E10), HA (F7), and GAPDH (6C5) from Santa Cruz Biotechnology, anti-Arp2/3-5 from Epitomics Inc. (Burlingame, CA), anti-coronin 1A from Everest Biotech Ltd. (Oxfordshire, UK), anti-CD28 Ab from BD Bioscience (San Jose, CA), and peroxidase-conjugated anti-rabbit IgG, anti-goat IgG, and anti-mouse IgG from DAKO-Japan (Tokyo). We obtained the pcDNA4-V5/His vector, pcDNA4-Myc/His vector, and SNARF-1 from Invitrogen and the pAcGFP1-N1 vector from Clontech Laboratories, Inc. HA-conjugated wild-type or mutated ubiquitin constructs were kind gifts from Dr. C. Akazawa at Tokyo Medical and Dental University. pAlter-MAX HA-Cbl-b was a kind gift from Dr. H. Band (University of Nebraska Medical Center).

Mice—DO11.10, OVA-specific TCR-transgenic mice were purchased from Jackson Laboratories. Seven-week-old female C57BL/6J mice were purchased from CLEA Laboratory Animal Corporation (Tokyo, Japan). The animals were maintained in specific pathogen-free conditions, and all care and use procedures were in accordance with institutional guidelines.

Cell Culture and Proliferation—DO11.10 splenocytes were cultured in complete DMEM (Invitrogen) supplemented with 0.05 mM 2-mercaptoethanol, 100 units/ml penicillin/streptomycin, and 10% FBS. Proliferative responses after 2 days of stimulation with plate-bound anti-CD3 (0.5 μg/ml) and anti-CD28 (1 μg/ml) Abs were determined by [^{3}H]thymidine incorporation using a β-1205 counter (Pharmacia). To induce anergy *in vitro*, DO11.10 splenocytes incubated with 1 mg/ml OVA for 3 days were rested for 7–10 days and were then stimulated for 18 h with ionomycin (1 μg/ml) (3).

Constructs—GRAIL, Arp2/3-5, coronin 1A, RhoGDIα, RhoGDIβ, Lasp1, and RGS10 cDNAs from DO11.10 T cells in which anergy had been induced by ionomycin were amplified with following the specific PCR primers: GRAIL, 5′-CAGTGAATTCATGGGGCCGCCGCCCGGGATC-3′ and 5′-CAGTCTCGAGAGATTTAATCTCCCGAACAGCAGC-3′; Arp2/3-5, 5′-CATGGAATTCTCCGGGATGTCGAAGAACACGGTGTC-3′ and 5′-GATCGCGGCCGCCACGGTTTTCCTTGCAGTCA-3′; coronin1A, 5′-GATCGCGGCCGCCTACTTGGCCTGAACAGTCT-3′ and 5′-CAGTCTCGAGCTTGGCCTGAACAGTCTCCTC-3′; RhoGDIα, 5′-CATGGAATTCGTAAGCATGGCAGAACAGGAACCCAC-3′ and 5′-GATCGCGGCCGCGTCCTTCCACTCCTTTTTGA-3′; RhoGDIβ, 5′-CATGGGATCCATCAAGATGACGGAGAAGGATGCACA-3′ and 5′-GATCGCGGCCGTTCTGTCCAATCCTTCTTAA-3′; and RGS10, 5′-CAGTGGATCCATGTTCACCCGCGCCGTG-3′ and 5′-CAGTCTCGAGTGTGTTGTAAATTCTGGAGGCTCG-3′. SOD1 cDNA from brain was amplified with the following PCR primers: 5′-CAGTGAATTCATGGCGATGAAAGCGGTGTGC-3′ and 5′-CAGTCTCGAGCTGCGCAATCCCAATCACTCC-3′. PCR products were cloned into a pcDNA4 V5/His vector or pcDNA4 Myc/His vector. The H297N and H300N mutations in the RING domain of murine GRAIL were generated using a PCR site-directed mutagenesis kit (Stratagene, Santa Clara, CA). Deletion of the RING domain in murine GRAIL was generated using the following PCR primers: for the 5′-PCR product, CAGTGAATTCATGGGGCCGCCGCCCGGGATC and CAGTTTCGAATCTCCATCAGGGCCAATTTC; and for the 3′-PCR product, CAGTTTCGAAGTGTGACATTCTCAAAGCT and CAGTCTCGAGAGATTTAATCTCCCGAACAGCAGC. After these reactions, the DNAs were digested with BamHI and HpaI, and the fragments, which were WT-GRAIL-V5/His, H2N2-GRAIL-V5/His, ΔRF-GRAIL-V5/His, Arp2/3-5-Myc/His, coronin 1A-Myc/His, RhoGDIα-Myc/His or RhoGDIβ-Myc/His, were subcloned into a pMIG vector. After pcDNA4 WT-GRAIL-V5/His was digested with NheI and XhoI, the fragment was subcloned into pAcGFP N1 vector.

Retroviral Transductions and Proliferation of Transfected T Cells—HEK293T cells were transfected with a pMIG plasmid and pCLEco helper plasmid by calcium phosphate precipitation. Supernatants were collected 48 and 72 h later and filtered through 0.45-μm syringe filters (Millipore, MA). Activated DO11.10 $CD4^+$T cells were resuspended in the collected supernatant (1×10^6 cells/ml) with recombinant IL-2 (50 units/ml) and polybrene (8 μg/ml) and were centrifuged at 2,500 rpm for 90 min. Transfected cells were expanded in complete DMEM with recombinant IL-2 for 48 h and were rested without IL-2. After treatment with ionomycin (0.3 μg/ml) for 18 h, the cells were stained with SNARF-1 (5 μM) for 15 min and were stimulated with plate-bound anti-CD3 and anti-CD28 Abs. Two days later, proliferation was analyzed using a FACSCalibur and the CELLQuest program (BD Biosciences).

Western Blot Analysis—The cells were washed with PBS and lysed in 1% Nonidet P-40 lysis buffer (137 mM NaCl, 1% Nonidet P-40, 10% glycerol, 20 mM Tris, pH 7.5). After incubation for 10 min on ice, lysates were centrifuged at 13,200 rpm for 15 min at 4 °C, and supernatants were collected. After adjustment of protein concentrations using the Dc protein assay (Bio-Rad), the lysates were mixed with Laemmli's buffer (1.33% SDS, 10% glycerol, 2% 2-mercaptoethanol, 0.002% bromphenol blue, 83 mM Tris, pH 6.8) and were boiled for 5 min. Lysates (10–30 μg) were subjected to 10 or 12% SDS-PAGE and immobilized on nitrocellulose membranes. The membranes were blocked with 5% milk, PBS, 0.05% Tween for 1 h at room temperature. Proteins were detected with various Abs (mostly diluted at 1:1000)

and horseradish peroxidase-coupled anti-rabbit, anti-mouse, or anti-goat IgG Abs (1:1000). The proteins were visualized using an enhanced chemiluminescence Western blot detection system (Amersham Biosciences).

Ubiquitination Assay—HEK293T cells were co-transfected with V5/His-tagged GRAIL, HA-tagged ubiquitin, and Myc/His-tagged substrate-containing expression vectors. Twenty-four hours later, the cells were incubated with 0.3 μM lactacystin for 12 h. The cells were lysed using 1% Nonidet P-40 lysis buffer containing protease inhibitors (Complete protease inhibitor mixture; Roche Applied Science) and were subjected to immunoprecipitation with anti-Myc Ab. Ubiquitination of substrates was analyzed by SDS-PAGE after blotting with anti-HA Ab.

Immunofluorescence Microscopy—To investigate co-localization of GRAIL and its substrates, HEK293T cells were co-transfected by calcium phosphate precipitation with the pAcGFP1-N1 vector containing GRAIL and pcDNA4-DsRed vector containing the substrate. Twenty-four hours later, the cells were incubated with lactacystin (0.3 μM) for 12 h and were fixed with MeOH for 15 min at 4 °C. To analyze T cell-B cell conjugation, A20 cells pulsed with 1 μg/ml $OVA_{323-339}$ for 2 h at 37 °C were incubated at a ratio of 1:1 with transfected GFP^+DO11.10 $CD4^+$T cells sorted on a FACS Aria cell sorter (BD Biosciences) at 37 °C for 10 min. The cells were then plated on poly-L-lysine-coated slides for 15 min. To analyze lamellipodium formation, T cells overexpressing the control or indicated constructs were settled onto anti-CD3-coated coverslips for 5 min as described previously (26). The cells were fixed with 4% paraformaldehyde for 15 min at 4 °C and washed with PBS, 0.01% Tween 20. After blocking with PBS, 1% BSA for 1 h at room temperature, the cells were incubated with either anti-Arp2/3-5 (C3) or anti-coronin 1A Ab for 18 h at 4 °C. After washing, the cells were labeled with Cy5-conjugated anti-mouse IgG or anti-goat IgG (Jackson ImmunoResearch Laboratories, West Grove, PA) for 2 h at room temperature. The slides were mounted with ProLong Gold antifade reagent (Invitrogen) with or without DAPI. Confocal images were acquired using FV1000-D (Olympus, Tokyo, Japan).

Statistical Analysis—Statistical differences between control and treatment groups were assessed with the Student's *t* test.

Additional Procedures—Information on semiquantitative RT-PCR and generation of shRNA is available in the supplemental materials.

RESULTS

Reduced Expression of Arp2/3-5 and Coronin 1A—E3 ubiquitin ligases including GRAIL are up-regulated in anergized T cells and play an important role in the induction of anergy (4, 8). To determine which proteins serve as substrates for GRAIL, we used two-dimensional difference gel electrophoresis to analyze proteins that were down-regulated in T cells in which anergy had been induced by ionomycin. Down-regulated proteins were identified by MALDI-TOF-MS and the nonredundant NCBI (NCBInr) database using MASCOT software (supplemental Table S1). Proteins related to cytoskeletal reorganization were the most frequently down-regulated proteins in anergic T cells. We decided to focus on actin-related proteins Arp2/3-5 and coronin 1A. We first confirmed that the expression levels of these proteins were reduced in T cells in ionomycin-induced anergy. We stimulated splenocytes of DO11.10 mice with OVA protein for 3 days and then rested them for 7 days. Anergy was induced by the addition of ionomycin for 18 h and the proliferative response upon the addition of anti-CD3 and anti-CD28 Abs detected by the incorporation of [^{3}H]thymidine. The proliferative response was significantly suppressed in ionomycin-treated cells, confirming that anergy was properly induced (Fig. 1*A*). In these anergized cells, the protein expression of Arp2/3-5 and coronin 1A was reduced (Fig. 1*B*, *lanes 2* and *4*). To address the functional involvement of Arp2/3-5 and coronin 1A in T cell anergy, we examined whether overexpression of these proteins in DO11.10 $CD4^+$ T cells enhanced their proliferative response upon stimulation. DO11.10 $CD4^+$ T cells were transfected with Arp2/3-5 or coronin 1A. To analyze proliferation of transfected T cells by flow cytometry, the cells were treated with ionomycin and labeled with SNARF-1, which can monitor proliferating cells through dye dilution in a similar fashion to CFSE dilution assay. The number of proliferating cells upon stimulation (GFP^+ $SNARF\text{-}1^-$ cells) was increased in Arp2/3-5 or coronin 1A-overexpressing cells compared with that of control cells (Fig. 1*C*). We also analyzed whether an anergy-like state was displayed by knockdown of Arp2/3-5 or coronin 1A. The percentage of proliferation increase upon the restimulation with anti-CD3/anti-CD28 was decreased in Arp2/3-5 shRNA-expressing T cells (8%) and in coronin 1A shRNA-expressing T cells (3%) compared with that in control shRNA-expressing cells (13%). These results indicate that the expression of Arp2/3-5 and coronin 1A is correlated with T cell responses and is reduced in anergic T cells.

GRAIL Polyubiquitinates Arp2/3-5 and Coronin 1A—We next examined whether Arp2/3-5 and coronin 1A serve as substrates for GRAIL. Myc-tagged Arp2/3-5, coronin 1A or other candidate substrate proteins were transiently co-expressed with V5-tagged GRAIL and HA-tagged ubiquitin (Ub) in HEK293T cells. Twenty-four hours after transfection, the cells were treated with the proteasome inhibitor lactacystin for 12 h, and then lysates were prepared and immunoprecipitated with an anti-Myc Ab. SDS-PAGE followed by immunoblotting with anti-HA revealed a polyubiquitinated laddering pattern of Arp2/3-5 and coronin 1A in the presence of GRAIL (Fig. 2*A*, *lanes 6* and *10*). As Rho GDP dissociation inhibitors (RhoGDI) α and β were previously reported as substrates of GRAIL, we confirmed that these two proteins were polyubiquitinated as well (Fig. 2*A*, *lanes 8* and *4*). On the other hand, Lasp1 (LIM and SH3 protein 1), RGS10 (regulator of G-protein signaling 10), and SOD1 (superoxide dismutase 1), which were identified as proteins with reduced expression in anergized T cells by the two-dimensional difference gel electrophoresis analysis, were not ubiquitinated in the presence of GRAIL (Fig. 2*A*, *lanes 2*, *12*, and *14*). These results indicate that Arp2/3-5 and coronin 1A are selectively polyubiquitinated by GRAIL. Histidine to asparagine substitution in the RING finger domain (H2N2) or deletion of the RING finger domain (ΔRF) of GRAIL (Fig. 2*B*) reportedly inactivates GRAIL. These mutant forms of GRAIL abrogated the ability of GRAIL to ubiquitinate Arp2/3-5 and coronin 1A as well as RhoGDIα and β (Fig. 2*C*). Recent evi-

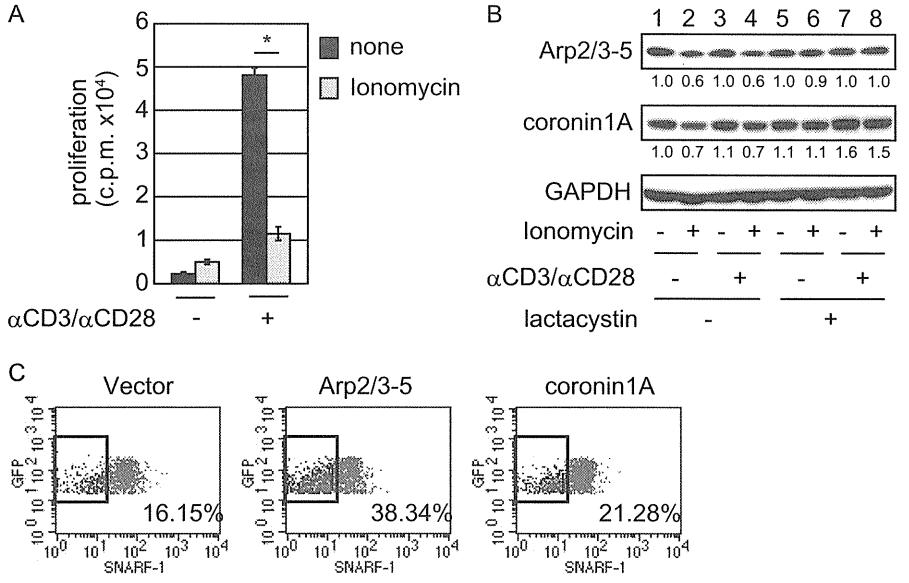

FIGURE 1. **Arp2/3-5 and coronin 1A are down-regulated in T cells anergized by ionomycin.** *A* and *B*, splenocytes derived from DO11.10 mice were stimulated with OVA for 3 days and rested for 7–10 days. The rested T cells were then treated with or without ionomycin for 18 h and restimulated with plate-bound anti-CD3 and soluble anti-CD28. *A*, proliferation was assessed by [^{3}H]thymidine uptake for 48 h. The mean c.p.m. of triplicate wells ± S.E. is shown (n = 9). *, p = 0.0000033 *versus* control. *B*, cells were lysed and analyzed by immunoblotting after 1-hour activation with plate-bound anti-CD3 and soluble anti-CD28. Each protein level analyzed by ImageJ software was normalized to the corresponding GAPDH level and is expressed as relative quantity to that of untreated control. *C*, DO11.10 CD4$^+$ T cells were transfected with vector control (GFP alone), Arp2/3-5, or coronin 1A. Forty-eight hours later, the transfected cells were treated with ionomycin for 18 h and were labeled with SNARF-1. The cells were restimulated with plate-bound anti-CD3 and soluble anti-CD28. Forty-eight hours later, proliferation was analyzed by FACS.

dence suggests that Cbl-b, which is E3 ligase as well as GRAIL, is important for induction of T cell anergy. We also analyzed whether Arp2/3-5 and coronin 1A are substrates of Cbl-b. However, Arp2/3-5 and coronin 1A are not ubiquitinated by Cbl-b (supplemental Fig. S1). These data indicate that GRAIL but not Cbl-b E3 ligase selectively ubiquitinates Arp2/3-5 and coronin 1A.

GRAIL Co-localizes with Arp2/3-5 and Coronin 1A—To address the interaction of Arp2/3-5 and coronin 1A with GRAIL, we examined the co-localization of these proteins. We transiently expressed GFP-tagged GRAIL together with HA-tagged ubiquitin and DsRed-tagged Arp2/3-5, coronin 1A, or RhoDGIα/β. After treatment with lactacystin, the localization of GRAIL and its substrates was analyzed by confocal microscopy. Indeed, Arp2/3-5 (Fig. 3*A*), coronin 1A (Fig. 3*B*), and RhoDGIα and β (Fig. 3, *C* and *D*) all co-localized with GRAIL. The substrates were localized together with GRAIL in contrast to the diffuse localization of GFP and substrate proteins in the cells transfected with GFP control vector and substrate proteins, indicating the co-localization of GRAIL and Arp2/3-5 or coronin 1A. These findings suggest that Arp2/3-5 and coronin 1A interact with GRAIL.

GRAIL Ubiquitinates Arp2/3-5 and Coronin 1A via Lys-63 and Lys-48—GRAIL has been reported to form polyubiquitin chains through lysine 63, resulting in proteolysis-independent functional modulation of Rho GDIs. However, when CD151 is the substrate, polyubiquitin chains are formed through lysine 48, which leads to protein degradation (18). We therefore assessed whether GRAIL ubiquitinates Arp2/3-5 and coronin 1A through Lys-63 and Lys-48. A similar polyubiquitinated ladder pattern of Arp2/3-5 was observed in the presence of WT Ub or Ub containing a lysine to arginine substitution at residue 29 (K29R) (Fig. 4*A*, *lanes 4* and *6*). In contrast, Ub conjugation of Arp2/3-5 was barely detected in the presence of Ub containing a lysine to arginine substitution at residue 48 (K48R) or at residue 63 (K63R) (Fig. 4*A*, *lanes 8* and *10*). Similarly, Ub conjugation of coronin 1A was observed in the presence of WT or K29R Ub (Fig. 4*B*, *lanes 4* and *6*) but was much lower when K48R or K63R Ub was used (Fig. 4*B*, *lanes 8* and *10*). These data reveal that Arp2/3-5 and coronin 1A were modified by Lys-48 and Lys-63 mixed linkage ubiquitin chains. To address the effect of GRAIL on the protein levels of Arp2/3-5 and coronin 1A, we overexpressed GRAIL and its enzymatically inactive mutant, H2N2-GRAIL or ΔRF-GRAIL, in DO11.10 CD4$^+$ T cells and determined Arp2/3-5 and coronin 1A expression by immunoblotting with specific Abs. Both Arp2/3-5 and coronin 1A were reduced when GRAIL, but not the enzymatically inactive forms of GRAIL, was overexpressed (Fig. 4*C*). These results indicate that GRAIL polyubiquitinates Arp2/3-5 and coronin 1A through Lys-48 and Lys-63 and eventually leads them to be degraded.

Less Arp2/3-5 and Coronin 1A Localize at the IS in Anergy—To investigate the role of Arp2/3-5 and coronin 1A in anergic T cells, we next examined the accumulation of F-actin, Arp2/3-5, and coronin 1A at the IS using confocal microscopy. As described previously, F-actin and Arp2/3-5 were recruited to the IS formed between DO11.10 CD4$^+$ T cells and $OVA_{323-339}$ peptide-pulsed A20 B cells (Fig. 5, *A* and *B*, *top panels*). In contrast, the accumulation of F-actin and the recruitment of Arp2/3-5 to the IS were reduced in ionomycin-treated DO11.10 CD4$^+$ T cells compared with those in control cells (Fig. 5*A*, *bottom panel*). Similarly, the recruitment of coronin 1A to the

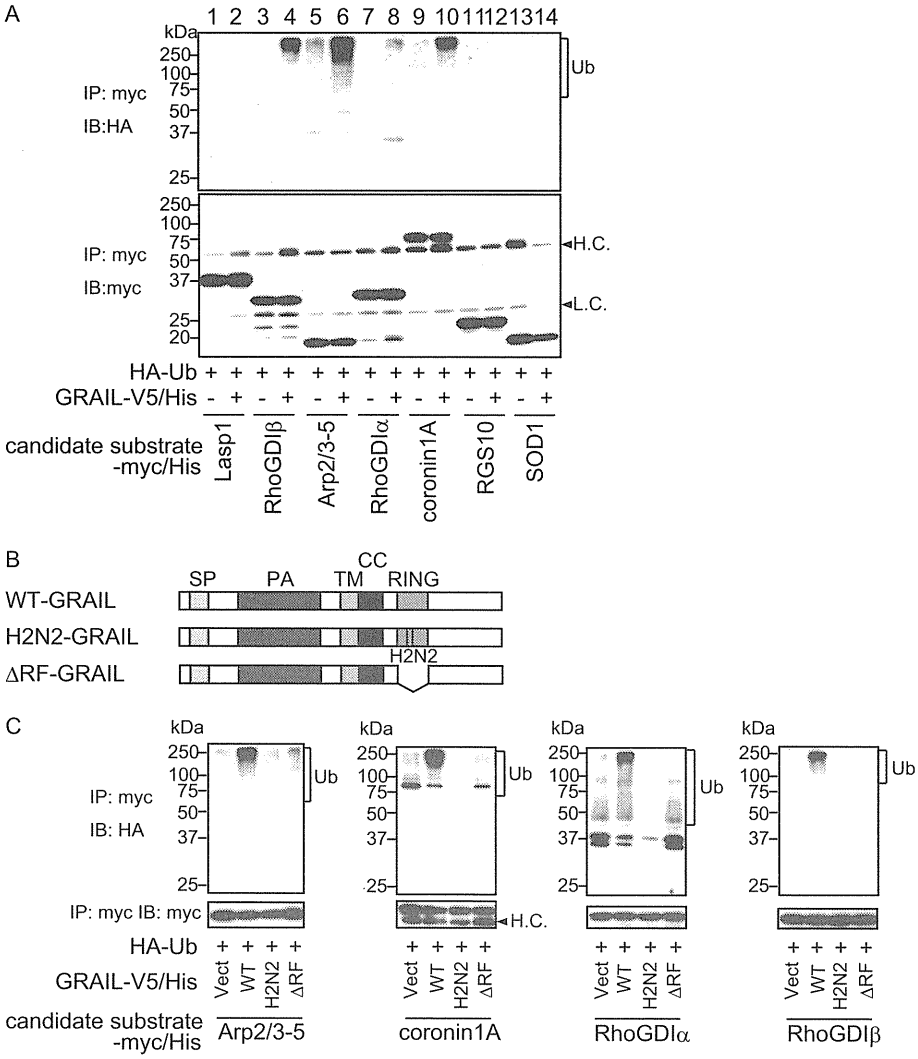

FIGURE 2. **Arp2/3-5 and coronin 1A are ubiquitinated by GRAIL.** *A* and *C*, HEK293T cells were transiently transfected with the indicated constructs and were treated with lactacystin for 12 h before lysis. Ubiquitination of the indicated proteins was detected by immunoprecipitation (*IP*) with anti-Myc Ab, followed by anti-HA immunoblotting (*IB*). The membrane was stripped and reprobed with anti-Myc Ab. *B*, schematic structures of the WT-, H2N2-, and ΔRF-GRAIL proteins.

IS in ionomycin-treated DO11.10 $CD4^+$ T cells was reduced compared with that in nontreated DO11.10 $CD4^+$ T cells (Fig. 5*B*, *bottom panel*). These data demonstrate that the accumulation of Arp2/3-5 and coronin 1A together with F-actin at the IS is impaired in anergic T cells.

GRAIL Inhibits Arp2/3 and Coronin 1A Accumulation at the IS—To address the contribution of GRAIL to IS formation, we overexpressed GRAIL, ΔRF-GRAIL, or a control vector in DO11.10 $CD4^+$ T cells and analyzed the accumulation of Arp2/3-5, coronin 1A, and F-actin at the IS. First, the expression of Arp2/3-5 and coronin 1A was reduced in T cells (GFP-positive cells) in which GRAIL was overexpressed compared with expression levels in control cells (Fig. 6, *A* and *B*, compare *top* and *middle panels*). The accumulation of both Arp2/3-5 and coronin 1A together with F-actin was reduced in DO11.10 $CD4^+$ T cells overexpressing GRAIL compared with that in control vector-transfected T cells (Fig. 6, *A* and *B*, compare *top* and *middle panels*). On the other hand, the accumulation of Arp2/3-5, coronin 1A, and F-actin at the IS in DO11.10 $CD4^+$ T cells overexpressing ΔRF-GRAIL was similar to that in controls (Fig. 6, *A* and *B*, *bottom panels*). We also examined whether the formation of IS occurred in ionomycin-treated T cells in which GRAIL was down-regulated by GRAIL shRNA-encoding retroviral infection. Coincident with the results for GRAIL-overexpressing experiments, both Arp2/3–5 and coronin 1A together with F-actin fully accumulated at the IS in ionomycin-treated GRAIL knockdown DO11.10 $CD4^+$ T cells compared with that in ionomycin-treated control T cells (anergic T cells) (supplemental Fig. S2). These results indicated that GRAIL regulates the recruitment of Arp2/3-5 and coronin 1A into the IS and the subsequent accumulation of F-actin at the site of the IS.

GRAIL Inhibits Lamellipodium Formation—Because Arp2/3 has been reported to be essential for the formation of lamellipodia at the IS, we next examined the effect of GRAIL on lamellipodium formation. Because the spreading of T cells on anti-TCR-coated coverslips requires the formation of stable actin structures and the generation of lamellipodia, we first analyzed whether T cells could spread onto anti-CD3-coated coverslips

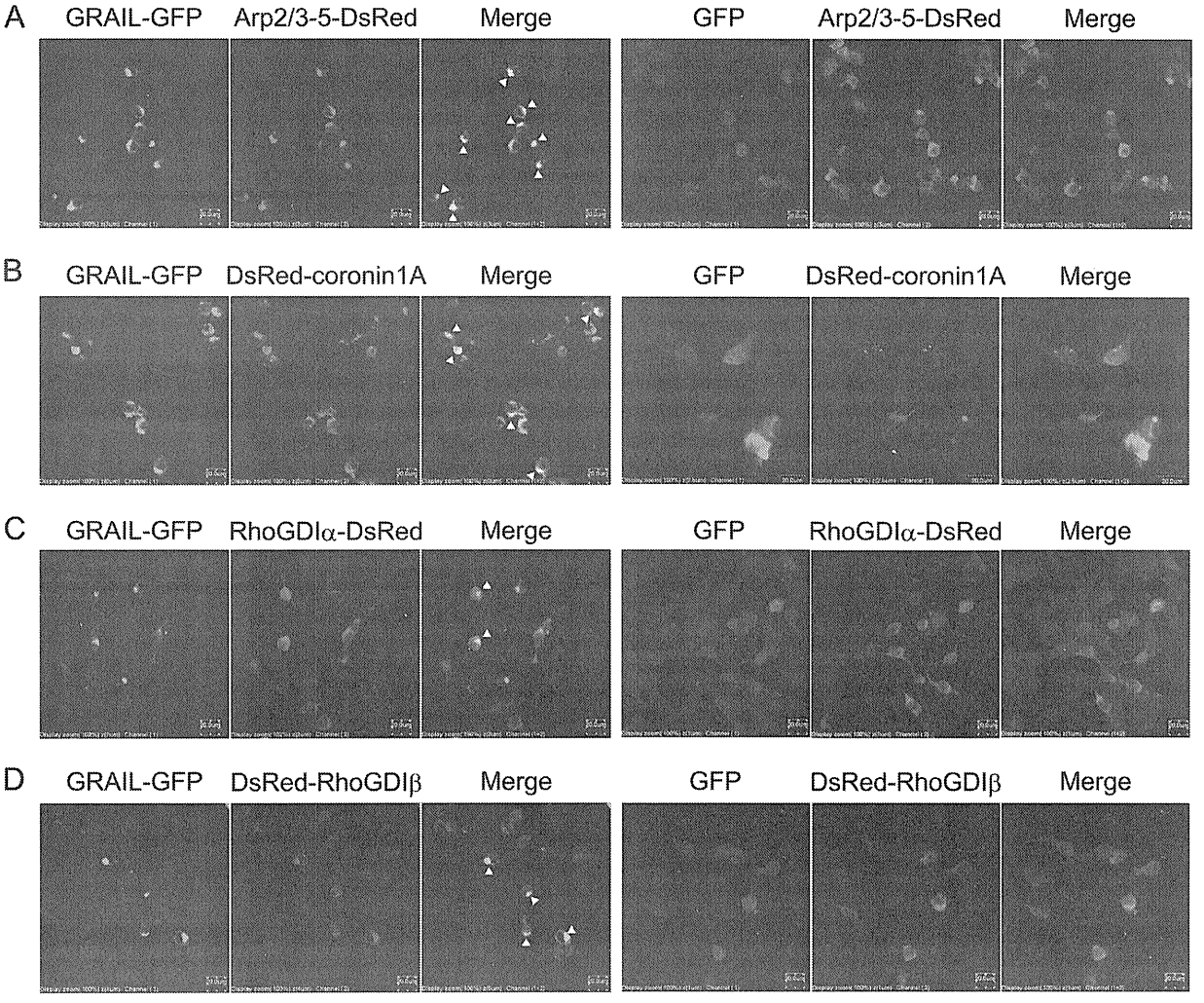

FIGURE 3. **GRAIL co-localizes with Arp2/3-5 and coronin 1A.** HEK293T cells were transiently transfected with constructs expressing GFP-tagged GRAIL, DsRed-tagged substrates (Arp2/3-5, *A*; coronin1A, *B*; RhoGDIα, *C*, and RhoGDIβ, *D*), and HA-ubiquitin and were treated with lactacystin for 12 h before being fixed. Co-localization with GFP-GRAIL was analyzed by confocal microscopy.

under anergic conditions. Control DO11.10 $CD4^+$ T cells spread onto anti-TCR-coated coverslips and formed round lamellipodial interfaces containing F-actin-rich structures (Fig. 7*A*). In contrast, DO11.10 $CD4^+$ T cells in which anergy had been induced by ionomycin barely formed lamellipodia (Fig. 7*A*, *bottom panels*). We next analyzed the lamellipodium formation in $CD4^+$ T cells overexpressing GRAIL. Lamellipodia were not efficiently formed on anti-CD3-coated coverslips when GRAIL was overexpressed in DO11.10 $CD4^+$ T cells (Fig. 7*B*, *middle panels*). In contrast, lamellipodia were efficiently formed at the IS when a catalytically inactive mutant GRAIL (ΔRF) was overexpressed in DO11.10 $CD4^+$ T cells (Fig. 7*B*, *bottom panels*). These data demonstrate that GRAIL inhibits lamellipodium formation at the IS.

DISCUSSION

In this study, we demonstrate that Arp2/3-5 and coronin 1A are down-regulated in anergic T cells as well as in T cells that overexpress GRAIL. Arp2/3-5 and coronin 1A co-localize with GRAIL and are ubiquitinated by GRAIL but not by Cbl-b via Lys-48 and Lys-63 linkage. Furthermore, the accumulation of Arp2/3-5 and coronin 1A together with F-actin is reduced at the IS in anergic T cells or in T cells that overexpress GRAIL. Coincident with the results for GRAIL-overexpressing experiments, IS formation in ionomycin-treated anergic T cells occurred by knockdown of GRAIL. Finally, we showed that overexpression of GRAIL suppresses lamellipodium formation at the IS.

CD40 ligand, CD151, CD83, and RhoGDI have been reported to be candidate substrates of GRAIL; however, the mechanism of GRAIL-mediated anergy induction is not yet fully understood (18–21). In fact, the expression of CD40 ligand was not up-regulated, and the down-regulation of CD3 was impaired in GRAIL-deficient mice. Because GRAIL is the only membrane protein among E3 ligases up-regulated in anergic T cells, it is reasonable that membrane proteins such as CD151 or CD83 are regulated by GRAIL. In this study, we confirmed that cytosolic proteins such as RhoGDIs serve as substrates for GRAIL. Fur-

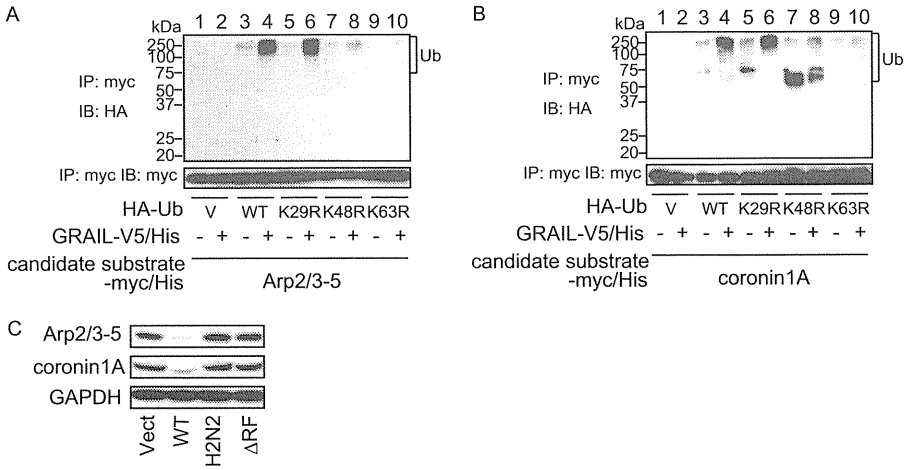

FIGURE 4. **Arp2/3-5 and coronin 1A are polyubiquitinated though Lys-48 and/or Lys-63 ubiquitin linkages and are down-regulated by catalytically active GRAIL.** *A* and *B*, HEK293T cells were transiently transfected with the indicated vectors and were treated with lactacystin for 12 h before lysis. Arp2/3-5 (*A*) and coronin 1A (*B*) were immunoprecipitated (*IP*) with anti-Myc Ab followed by immunoblotting (*IB*) with anti-HA Ab. The membrane was stripped and reprobed with anti-Myc Ab. *C*, $CD4^+$ T cells were transfected with vector control (GFP alone) or WT-, H2N2-, or ΔRF-GRAIL expression constructs. Forty-eight hours later, the transfected cells (GFP^+ cells) were sorted using a FACS Aria cell sorter. Sorted cells were rested for 2 days and were subjected to immunoblot analysis with anti-coronin 1A or Arp2/3-5 Ab.

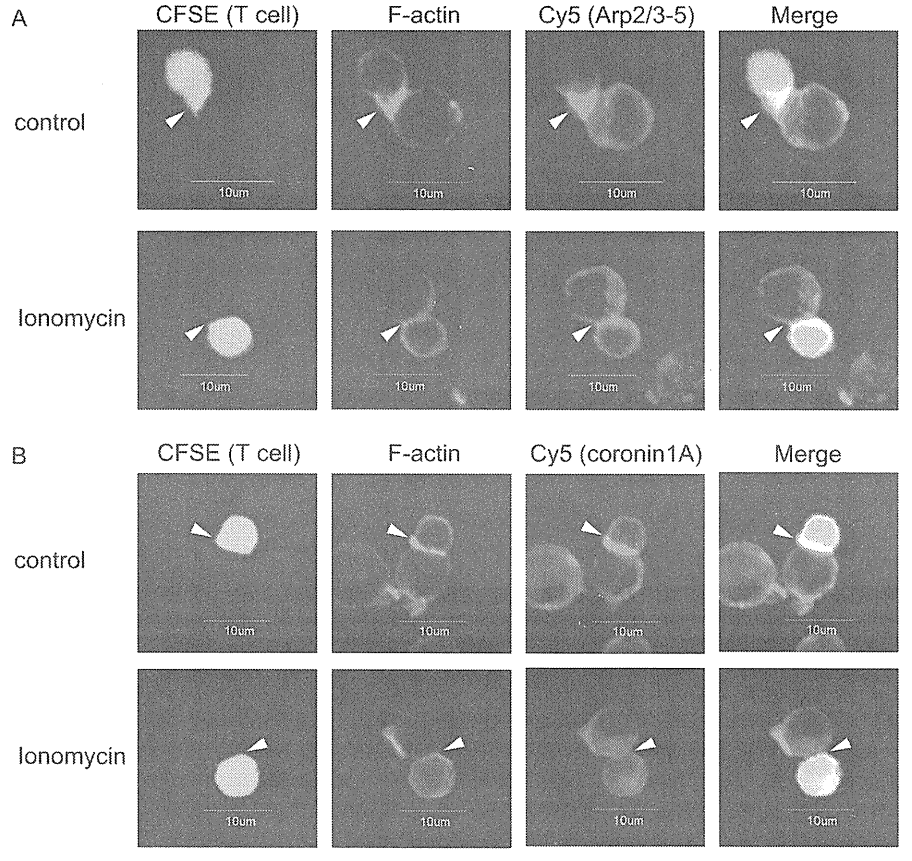

FIGURE 5. **The accumulation of Arp2/3-5, coronin 1A, and F-actin at the IS is reduced in anergic T cells.** *A* and *B*, OVA-stimulated DO11.10 splenocytes were rested for 7–10 days. Rested T cells were stained with CFSE, treated with or without ionomycin for 18 h, incubated with $OVA_{323-339}$-pulsed A20 cells, and co-stained with rhodamine-phalloidin (*red*) to visualize F-actin and either anti-Arp2/3-5 Ab (*A*) or anti-coronin 1A Ab (*purple*) (*B*). The *arrowheads* indicate IS.

thermore, we identified Arp2/3-5 and coronin 1A as novel substrates for GRAIL. Interestingly, these proteins as well as RhoGDIs are reportedly involved in the regulation of cytoskeletal organization. Although ubiquitination of target proteins was almost completely lost when either K63R or K48R mutant ubiquitin was used, it remains unclear whether Arp2/3-5 and coronin 1A are ubiquitinated via Lys-48, Lys-63, or both sites. To address this issue, characterization of ubiquitin chain using

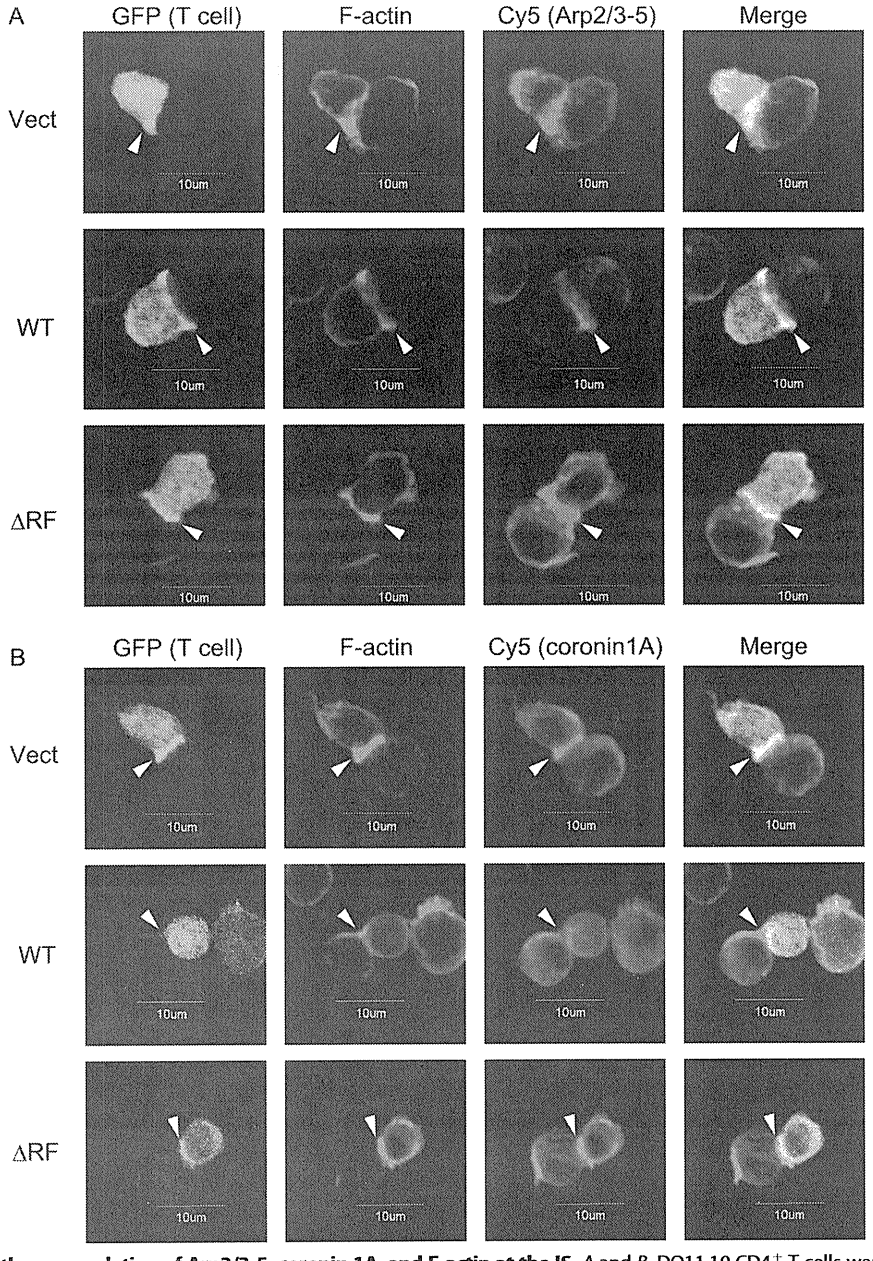

FIGURE 6. **GRAIL inhibits the accumulation of Arp2/3-5, coronin 1A, and F-actin at the IS.** *A* and *B*, DO11.10 CD4$^+$ T cells were transfected with vector control (GFP alone) or WT- or ΔRF-GRAIL expression constructs (*green*). Each population was incubated with $OVA_{323-339}$-pulsed A20 cells and co-stained with rhodamine-phalloidin (*red*) and either anti-Arp2/3-5 (*A*) or anti-coronin 1A (*purple*) (*B*). The *arrowheads* indicate IS.

MALDI-TOF-MS or mutants in which Lys-48 or Lys-63 is the only lysine residue that can mediate the ubiquitin chain formation will be needed for future studies

The immunological synapse is important in sustained signaling and delivery of a subset of effector cytokines by CD4$^+$ T cells (25, 29, 31, 32). Although the precise contribution of actin cytoskeletal remodeling to T cell signaling and biologic function is not completely understood, both anergic T cells and T cells overexpressing GRAIL have been reported to form unstable immunologic synapses (4, 38). Actin nucleation in T cells is induced by the WAVE2 complex (33) and the actin-nucleation-promoting factor WASPs, which are required to promote and stabilize interactions between T cells and APC *in vitro* and TCR clustering on artificial surfaces. WASPs bind to actin monomers, whereas the acidic stretch associates with the Arp2/3-5 complex (23, 34), a seven-subunit complex that has intrinsic actin-nucleating activity and is essential for polarization of F-actin at the IS (25, 35). In addition, co-localization of WASPs and the Arp2/3-5 complex at the interface between anti-CD3-coated beads and Jurkat T cells suggests that these cytoskeletal components are essential for the dynamics of the actin cytoskeleton and for T cell function (24). Arp2/3-5 is essential for the formation of a stable synapse by creating lamellipodia (25). Consistent with these findings, overexpression of GRAIL reduced the protein expression of Arp2/3-5 and impaired lamellipodium formation. These results suggest that proteins

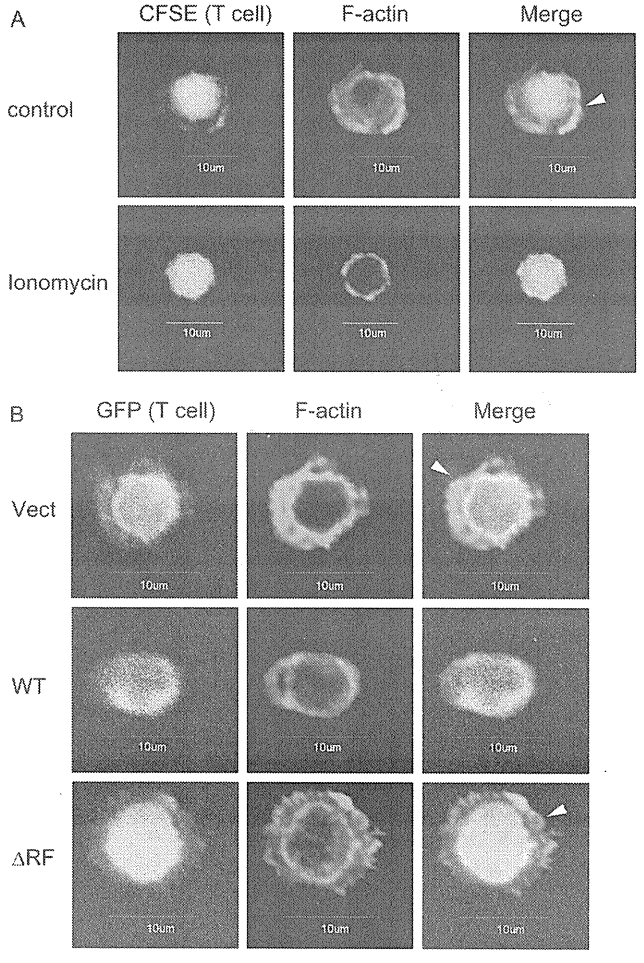

FIGURE 7. **GRAIL inhibits lamellipodium formation during TCR stimulation.** *A*, OVA-stimulated DO11.10 splenocytes were rested for 7–10 days and stained with CFSE. The cells were treated with or without ionomycin for 18 h. The cells were stimulated with plate-bound anti-CD3 mAb and stained with rhodamine-phalloidin (*red*) to visualize F-actin. *B*, DO11.10 $CD4^+$ T cells were transfected with a control vector (GFP alone) or WT- or ΔRF-GRAIL expression vectors. The cells were stimulated with coated anti-CD3 mAb and stained with rhodamine-phalloidin (*red*). The *arrowheads* indicate lamellipodium formation.

related to cytoskeletal reorganization at the IS are cytosolic targets for GRAIL.

An earlier study of coronin 1A knock-out mice reported that coronin 1A has an Arp2/3-5-dependent inhibitory effect on F-actin formation and concluded that coronin 1A is indispensable for TCR signaling (27, 29). In the present study, overexpression of coronin 1A restored the proliferative response. These findings suggest that coronin 1A participates in modulating T cell signaling and thereby contributes to the maintenance of anergy. In anergic T cells and in T cells overexpressing GRAIL, F-actin accumulation at the IS was decreased, although the expression of coronin 1A was reduced in contrast to previous studies. This may be because GRAIL regulates not only coronin 1A but also the Arp2/3-5 complex as well as RhoGDIs, which are important in the regulation of the accumulation of F-actin.

Anergic T cells have been reported to exhibit initial interaction, but implementation of T cell anergy results in reduced binding of LFA-1 to its ligand ICAM-1 (4). This process is mediated through degradation of PKC-θ and phospholipase C-γ by Cbl-b. A recent report demonstrated that overexpression of GRAIL impairs LFA-1 polarization at the IS (37). Stimulation through the TCR was shown to result in WAVE2-Arp2/3-5-dependent F-actin nucleation and the formation of a complex containing WAVE2, Arp2/3-5, vinculin, and talin (33). Moreover, TCR stimulation induces integrin clustering through the recruitment of vinculin and talin (33). Therefore, our study might link the unstable immunological synapse formation and impaired LFA-1 polarization at the IS in anergic T cells. Thus, whereas Cbl-b leads to unstable immunological synapse through degradation of tyrosine kinase, GRAIL leads to the phenotype of synapse disorganization via degradation of proteins involved in the actin cytoskeletal organization. In summary, we provide evidence that GRAIL regulates cytoskeletal reorganization to keep cells unresponsive to further antigen stimulation through the ubiquitination and down-regulation of the Arp2/3-5 complex and coronin 1A.

REFERENCES

1. Schwartz, R. H. (2003) *Annu. Rev. Immunol.* **21,** 305–334
2. Walker, L. S., and Abbas, A. K. (2002) *Nat. Rev. Immunol.* **2,** 11–19
3. Quill, H., and Schwartz, R. H. (1987) *J. Immunol.* **138,** 3704–3712
4. Heissmeyer, V., Macián, F., Im, S. H., Varma, R., Feske, S., Venuprasad, K., Gu, H., Liu, Y. C., Dustin, M. L., and Rao, A. (2004) *Nat. Immunol.* **5,** 255–265
5. Jeon, M. S., Atfield, A., Venuprasad, K., Krawczyk, C., Sarao, R., Elly, C., Yang, C., Arya, S., Bachmaier, K., Su, L., Bouchard, D., Jones, R., Gronski, M., Ohashi, P., Wada, T., Bloom, D., Fathman, C. G., Liu, Y. C., and Penninger, J. M. (2004) *Immunity* **21,** 167–177
6. Venuprasad, K., Elly, C., Gao, M., Salek-Ardakani, S., Harada, Y., Luo, J. L., Yang, C., Croft, M., Inoue, K., Karin, M., and Liu, Y. C. (2006) *J. Clin. Invest.* **116,** 1117–1126
7. Hsiao, H. W., Liu, W. H., Wang, C. J., Lo, Y. H., Wu, Y. H., Jiang, S. T., and Lai, M. Z. (2009) *Immunity* **31,** 72–83
8. Anandasabapathy, N., Ford, G. S., Bloom, D., Holness, C., Paragas, V., Seroogy, C., Skrenta, H., Hollenhorst, M., Fathman, C. G., and Soares, L. (2003) *Immunity* **18,** 535–547
9. Andoniou, C. E., Lill, N. L., Thien, C. B., Lupher, M. L., Jr., Ota, S., Bowtell, D. D., Scaife, R. M., Langdon, W. Y., and Band, H. (2000) *Mol. Cell Biol.* **20,** 851–867
10. Rao, N., Miyake, S., Reddi, A. L., Douillard, P., Ghosh, A. K., Dodge, I. L., Zhou, P., Fernandes, N. D., and Band, H. (2002) *Proc. Natl. Acad. Sci. U.S.A.* **99,** 3794–3799
11. Lupher, M. L., Jr., Rao, N., Lill, N. L., Andoniou, C. E., Miyake, S., Clark, E. A., Druker, B., and Band, H. (1998) *J. Biol. Chem.* **273,** 35273–35281
12. Lupher, M. L., Jr., Songyang, Z., Shoelson, S., Cantley, L. C., and Band, H. (1997) *J. Biol. Chem.* **272,** 33140–33144
13. Duan, L., Reddi, A. L., Ghosh, A., Dimri, M., and Band, H. (2004) *Immunity* **21,** 7–17
14. Fang, D., and Liu, Y. C. (2001) *Nat. Immunol.* **2,** 870–875
15. Liu, Y. C. (2004) *Annu. Rev. Immunol.* **22,** 81–127
16. Kriegel, M. A., Rathinam, C., and Flavell, R. A. (2009) *Proc. Natl. Acad. Sci. U.S.A.* **106,** 16770–16775
17. Nurieva, R. I., Zheng, S., Jin, W., Chung, Y., Zhang, Y., Martinez, G. J., Reynolds, J. M., Wang, S. L., Lin, X., Sun, S. C., Lozano, G., and Dong, C. (2010) *Immunity* **32,** 670–680
18. Lineberry, N. B., Su, L. L., Lin, J. T., Coffey, G. P., Seroogy, C. M., and Fathman, C. G. (2008) *J. Immunol.* **181,** 1622–1626
19. Lineberry, N., Su, L., Soares, L., and Fathman, C. G. (2008) *J. Biol. Chem.* **283,** 28497–28505
20. Su, L. L., Iwai, H., Lin, J. T., and Fathman, C. G. (2009) *J. Immunol.* **183,** 438–444

21. Su, L., Lineberry, N., Huh, Y., Soares, L., and Fathman, C. G. (2006) *J. Immunol.* **177,** 7559–7566
22. Holsinger, L. J., Graef, I. A., Swat, W., Chi, T., Bautista, D. M., Davidson, L., Lewis, R. S., Alt, F. W., and Crabtree, G. R. (1998) *Curr. Biol.* **8,** 563–572
23. Machesky, L. M., and Insall, R. H. (1998) *Curr. Biol.* **8,** 1347–1356
24. Krause, M., Sechi, A. S., Konradt, M., Monner, D., Gertler, F. B., and Wehland, J. (2000) *J. Cell Biol.* **149,** 181–194
25. Gomez, T. S., Kumar, K., Medeiros, R. B., Shimizu, Y., Leibson, P. J., and Billadeau, D. D. (2007) *Immunity* **26,** 177–190
26. Nolz, J. C., Gomez, T. S., Zhu, P., Li, S., Medeiros, R. B., Shimizu, Y., Burkhardt, J. K., Freedman, B. D., and Billadeau, D. D. (2006) *Curr. Biol.* **16,** 24–34
27. Föger, N., Rangell, L., Danilenko, D. M., and Chan, A. C. (2006) *Science* **313,** 839–842
28. Rodal, A. A., Sokolova, O., Robins, D. B., Daugherty, K. M., Hippenmeyer, S., Riezman, H., Grigorieff, N., and Goode, B. L. (2005) *Nat. Struct. Mol. Biol.* **12,** 26–31
29. Mugnier, B., Nal, B., Verthuy, C., Boyer, C., Lam, D., Chasson, L., Nieoullon, V., Chazal, G., Guo, X. J., He, H. T., Rueff-Juy, D., Alcover, A., and Ferrier, P. (2008) *PLos One.* **3,** e3467
30. Haraldsson, M. K., Louis-Dit-Sully, C. A., Lawson, B. R., Sternik, G., Santiago-Raber, M. L., Gascoigne, N. R., Theofilopoulos, A. N., and Kono, D. H. (2008) *Immunity.* **28,** 40–51
31. Bachmaier, K., Krawczyk, C., Kozieradzki, I., Kong, Y. Y., Sasaki, T., Oliveira-dos-Santos, A., Mariathasan, S., Bouchard, D., Wakeham, A., Itie, A., Le, J., Ohashi, P. S., Sarosi, I., Nishina, H., Lipkowitz, S., and Penninger, J. M. (2000) *Nature.* **403,** 211–216
32. Fang, D., Wang, H. Y., Fang, N., Altman, Y., Elly, C., and Liu, Y. C. (2001) *J. Biol. Chem.* **276,** 4872–4878
33. Nolz, J. C., Medeiros, R. B., Mitchell, J. S., Zhu, P., Freedman, B. D., Shimizu, Y., and Billadeau, D. D. (2007) *Mol. Cell Biol.* **27,** 5986–6000
34. Miki, H., Miura, K., and Takenawa, T. (1996) *EMBO J.* **15,** 5326–5335
35. Goley, E. D., and Welch, M. D. (2006) *Nat. Rev. Mol. Cell Biol.* **7,** 713–726
36. Deleted in proof
37. Schartner, J. M., Simonson, W. T., Wernimont, S. A., Nettenstrom, L. M., Huttenlocher, A., and Seroogy, C. M. (2009) *J. Biol. Chem.* **284,** 34674–34681
38. Mueller, P., Massner, J., Jayachandran, R., Combaluzier, B., Albrecht, I., Gatfield, J., Blum, C., Ceredig, R., Rodewald, H. R., Rolink, A. G., and Pieters, J. (2008) *Nat. Immunol.* **9,** 424–431

Cellular Immunology 266 (2011) 165–171

Contents lists available at ScienceDirect

Cellular Immunology

journal homepage: www.elsevier.com/locate/ycimm

The role of tumor necrosis factor-α for interleukin-10 production by murine dendritic cells

Noriyuki Hirata [a,b], Yoshiki Yanagawa [a,c,*], Hisako Ogura [a], Masashi Satoh [a], Masayuki Noguchi [b], Machiko Matsumoto [c], Hiroko Togashi [c], Kazunori Onoé [a], Kazuya Iwabuchi [a]

[a] Division of Immunobiology, Institute for Genetic Medicine, Hokkaido University, West 7 North 15, Sapporo 060-0815, Japan
[b] Division of Cancer Biology, Institute for Genetic Medicine, Hokkaido University, West 7 North 15, Sapporo 060-0815, Japan
[c] Department of Pharmacology, Faculty of Pharmaceutical Science, Health Sciences University of Hokkaido, Kanazawa 1757, Ishikari-Tobetsu 060-0293, Japan

ARTICLE INFO

Article history:
Received 9 June 2010
Accepted 30 September 2010
Available online 8 October 2010

Keywords:
Dendritic cells
Interleukin-10
Signal transduction
Tumor necrosis factor-α
Toll-like receptor

ABSTRACT

In the present study, we examined the role of tumor necrosis factor (TNF) in interleukin (IL)-10 production by dendritic cells (DCs) using bone-marrow derived DCs from wild type (WT) and TNF-α knockout (TNF-$\alpha^{-/-}$) mice. Toll-like receptor (TLR) stimulation induced substantial level of IL-10 production by WT DCs, but significantly low level of IL-10 production by TNF-$\alpha^{-/-}$ DCs. In contrast, no significant difference was detected in IL-12 p40 production between WT and TNF-$\alpha^{-/-}$ DCs. Addition of TNF-α during TLR stimulation recovered the impaired ability of TNF-$\alpha^{-/-}$ DCs for IL-10 production. This recovery appeared to be associated with an activation of extracellular signal-regulated kinase, p38 mitogen-activated protein kinase, and phosphatidylinositol 3-kinase/Akt following the TNF-α addition. Blocking these kinases significantly inhibited IL-10 production by TNF-$\alpha^{-/-}$ DCs stimulated with TLR ligands plus TNF-α. Thus, TNF-α may be a key molecule to regulate the balance between anti-inflammatory versus inflammatory cytokine production in DCs.

1. Introduction

Tumor necrosis factor (TNF)-α is a multifunctional cytokine that regulates immunity, inflammation, cell differentiation, proliferation, and apoptosis [1,2]. TNF-α binds to two distinct receptors, TNF receptor type 1 (TNFR1; CD120a) and TNF receptor type 2 (TNFR2; CD120b) [3]. Most of TNF functions are thought to be induced via TNFR1. TNFR1 is constitutively expressed in most tissues. TNFR1 recruits death-domain proteins including TNFR1-associated death domain protein (TRADD) and Fas-associated death domain proteins (FADDs) [4]. TRADD activates FADDs, receptor-interacting protein 1 (RIP1), and TNF receptor-associated factor 2 (TRAF2). TRAF2 and RIP1 activate mitogen-activated protein kinases (MAPKs), such as extracellular signal-regulated kinase (ERK), p38 MAPK, c-jun amino-terminal kinases (JNK), and nuclear factor-κB (NF-κB) [1,2,5–7].

Toll-like receptors (TLRs) are pattern recognition receptors that recognize pathogen-associated molecular patterns (PAMPs) in the pathogen-derived molecules such as lipopolysaccharide (LPS) and induce innate immune responses. The TLR family consists of more than 13 members in mammals [8]. TLRs recognize various PAMPs, such as lipoproteins (TLR2), peptidoglycan (TLR2), double-stranded RNA (TLR3), LPS (TLR4), flagellin (TLR5), single-stranded RNA (TLR7 and TLR8), and CpG-DNA (TLR9). TLRs contain a Toll-IL-1R (TIR) domain [9,10]. Upon TLR activation, TIR domain efficiently recruits several TIR-containing intracellular adaptor proteins including myeloid differentiation primary-response gene 88 (MyD88) [11,12] and TIR domain-containing adaptor inducing interferon (IFN)-β (TRIF) [13,14]. The MyD88-dependent signaling pathway activates MAPKs, NF-κB, phosphatidylinositol 3-kinase (PI3K)/Akt, activator protein-1, and IFN regulatory factor (IRF) 5 via

Abbreviations: Ab, antibody; BMDCs, bone marrow-derived dendritic cells; DCs, dendritic cells; ELISA, enzyme linked immunosorbent assay; ERK, extracellular signal-regulated kinase; FADD, Fas-associated death domain protein; FCS, fetal calf serum; FITC, fluorescein isothiocyanate; GM-CSF, granulocyte-macrophage colony-stimulating factor; h, hour; JNK, c-jun N-terminal kinase; IFN, interferon; IL, interleukin; IRF, IFN regulatory factor; LPS, lipopolysaccharide; mAb, monoclonal Ab; MAPK, mitogen-activated protein kinase; MEK, MAPK/ERK kinase; min, minute; MyD88, myeloid differentiation primary-response gene 88; NF-κB, nuclear factor-κB; pAkt, phospho-Akt; PAMPs, pathogen-associated molecular patterns; P3C, Pam3CSK4; PI3K, phosphatidylinositol 3-kinase; PE, phycoerythrin; PerCP, peridinin chlorophyll protein; pERK, phospho-ERK; pJNK, phospho-JNK; pp38 MAPK, phospho-p38 MAPK; Th1, T helper type 1; TLR, Toll-like receptor; TLR-L, TLR ligands; TNF, tumor necrosis factor; TNFR1, TNF receptor type 1; TNFR2, TNF receptor type 2; TRADD, TNFR1-associated death domain protein; TRAF, TNF receptor-associated factor; TRIF, TIR domain-containing adaptor inducing IFN-β; WT, wild type.

* Corresponding author at: Department of Pharmacology, Faculty of Pharmaceutical Science, Health Sciences University of Hokkaido, Kanazawa 1757, Ishikari-Tobetsu 060-0293, Japan. Fax: +81 133 23 1579.
E-mail address: yanagawa@hoku-iryo-u.ac.jp (Y. Yanagawa).

0008-8749/$ - see front matter © 2010 Elsevier Inc. All rights reserved.
doi:10.1016/j.cellimm.2010.09.012

TRAF6, which induces inflammatory cytokine synthesis. The TRIF-dependent signaling pathway activates IRF3, IRF7, and NF-κB via RIP1, TRAF3, and TRAF6, which induces type I IFNs [10,15–19].

Dendritic cells (DCs) are potent professional antigen-presenting cells and play important roles in the initiation and the regulation of immune responses to various pathogenic antigens [20–22]. TLR-stimulated DCs produce a large amount of inflammatory cytokines including TNF-α, interleukin (IL)-1, IL-6, and IL-12 and also anti-inflammatory cytokines such as IL-10. DC-produced IL-12 drives polarization of naïve $CD4^+$ T cells toward T helper type 1 (Th1) cells, while the IL-10 is involved in inhibition of Th1 responses and differentiation of regulatory T cells [23–26]. It seems that the balance of inflammatory versus anti-inflammatory cytokines produced by DCs is crucial to control immune homeostasis. However, the mechanism underlying regulation of the cytokine balance has not been fully understood.

TNF-α exhibits not only pro-inflammatory functions but also displays anti-inflammatory properties [27–29]. It has been reported that TNF-α promotes IL-10 production by human monocytes [30,31], although molecular mechanism underlying the TNF-α-mediated regulation of IL-10 production remains unclear. On the other hand, the role of TNF-α for IL-10 production by DCs has not been well documented. In the present study, using bone-marrow derived DCs (BMDCs) generated from either wild type (WT) or TNF-α knockout (TNF-$\alpha^{-/-}$) mice, we examined the role of TNF-α in DC production of IL-10 upon TLR stimulation focusing on the intracellular signaling.

2. Materials and methods

2.1. Mice

WT C57BL/6 mice were purchased from Japan SLC (Hamamatsu, Japan). TNF-α knockout (TNF-$\alpha^{-/-}$) mice with C57BL/6 background were obtained from The Jackson Laboratory (Bar Harbor, ME). All mice were maintained in a specific pathogen-free condition of our animal facility at Hokkaido University. Female mice at 6- to 14-weeks old were used for the preparation of bone marrow cells. All experiments were approved by regulations of Hokkaido University Animal Care and Use Committee.

2.2. Reagents and antibodies (Abs)

Murine recombinant granulocyte–macrophage colony-stimulating factor (GM-CSF) and murine recombinant TNF-α were purchased from PeproTech (Rocky Hill, NJ). Rabbit complement was purchased from Cedarlane (Ontario, Canada). LPS (ultra-pure grade) from *Escherichia coli* (O111:B4) and Pam3CSK4 (P3C), a synthetic lipopeptide, were purchased from Invivogen (San Diego, CA). Fluorescein isothiocyanate (FITC)-conjugated anti-mouse CD86 monoclonal Ab (mAb) (GL1), phycoerythrin (PE)-conjugated anti-mouse CD40 mAb (3/23), biotin-conjugated anti-I-A^b mAb (AF6-120.1), and streptavidin–peridinin chlorophyll protein (PerCP) were obtained from BD Pharmingen (San Jose, CA). Anti-mouse TNF-α mAb (MP6-XT22), anti-mouse TNFR1 mAb (55R-170), and anti-mouse TNFR2 mAb (TR75-54.7) were purchased from Biolegend (San Diego, CA). Anti-phospho-ERK1/2 (Thr^{202}/Tyr^{204}) mAb (197G2), anti-phospho-p38 MAPK (Thr^{180}/Tyr^{182}) Ab, anti-phospho-JNK1/2 (Thr^{183}/Tyr^{185}) mAb (G9), anti-phospho-Akt (Ser^{473}) mAb (193H12), and anti-GAPDH mAb (14C10) were purchased from Cell Signaling Technology (Beverly, MA). U0126, a specific inhibitor of MAPK/ERK kinase (MEK)1/2, and SB203580, a specific inhibitor of p38 MAPK, were purchased from Calbiochem (San Diego, CA). LY294002, a specific inhibitor of PI3K, was purchased from Sigma–Aldrich (St. Louis, MO).

2.3. Generation of BMDCs

Murine BMDCs were generated by a well established method as previously described [32,33] with a minor modification. Bone marrow cells were prepared from femur and tibial bone marrow of WT or TNF-$\alpha^{-/-}$ mice. After lysis of erythrocytes, major histocompatibility complex class II-, CD45R (B220)-, CD4-, and CD8-positive cells were removed by killing with a cocktail of relevant mAbs (1E4, RA3-6B2, GK1.5, and 53–6.7) and rabbit complement. The cells were extensively washed to remove mAbs, complement, and cell debris. The cells were cultured in RPMI-1640 containing 5% fetal calf serum (FCS) and GM-CSF (20 ng/ml) at a density of 1×10^6 cells/ml/well (24-well plate). On day 2, the medium was gently exchanged to fresh medium. On day 4, non-adherent granulocytes were removed without dislodging clusters of developing DCs, and fresh medium was added. On day 6, free-floating and loosely adherent cells were collected and were used as BMDCs (>95% $CD11c^+$ $B220^-$).

2.4. Measurement of cytokines in culture supernatants

BMDCs (2×10^5/ml) were treated with TNF-α and/or P3C (100 ng/ml) plus LPS (1 μg/ml) (this combination of TLR ligands will be referred to as TLR-L) for 24 h in 5% FCS RPMI-1640 [34]. TNF-α was used at 100 ng/ml based on our preliminary dose–response study (data not shown). In some experiments, cells (2×10^5/ml) were pretreated with U0126, SB203580, LY294002, or vehicle alone (0.1% DMSO) for 1 h and then stimulated with TNF-α and/or TLR-L for 24 h in the presence of each inhibitor. U0126, SB203580, and LY294002 were used at 10, 30, and 10 μM, respectively, as previously described [34]. The culture supernatants were subjected to quantification of the protein level of IL-10, IL-12 p40, and TNF-α by enzyme linked immunosorbent assay (ELISA) using OptEIA Set (BD Pharmingen).

2.5. Immunoblotting

BMDCs (5×10^5/ml) were treated with TLR-L and/or TNF-α for 24 h in 5% FCS RPMI-1640 for the indicated time period. Reactions were halted by rapidly cooling on ice, and these cells were washed by ice-cold phosphate-buffered saline. The whole cell lysates were prepared using cell lysis buffer (Cell signaling Technology). The cell lysates were separated by sodium dodecyl sulfate–polyacrylamide gel electrophoresis, and then blotted onto a polyvinylidene fluoride membrane (Millipore, Bedford, MA). The membrane were proved with primary Ab, and developed with horseradish peroxidase-conjugated secondary Ab by enhanced chemiluminescence.

2.6. Flow cytometry

Cell staining with FITC-, PE-, or biotin-conjugated mAb, and streptavidin-PerCP and flow cytometric analysis was performed on EPICS XL (Beckman coulter Inc., Miami, FL) as previously described [35].

2.7. Statistical analysis

The Student's *t*-test or Dunnet's test was used to analyze data for significant differences. *P* values less than 0.05 were regarded as significant.

3. Results

3.1. Cytokine production by WT and TNF-$\alpha^{-/-}$ DCs upon TLR stimulation

We examined the role of endogenous TNF-α in IL-10 production by murine BMDCs in response to TLR ligands comparing BMDCs

from TNF-$\alpha^{-/-}$ mice and those from WT mice. We have previously demonstrated that LPS (ultra-pure grade) or P3C (a synthetic TLR2 ligand) alone induced negligible production of IL-10 in BMDCs, while the simultaneous treatment with these ligands results in the vigorous production of IL-10 [34]. Thus, DCs were stimulated with LPS plus P3C to evaluate the ability for the IL-10 production.

BMDCs from WT or TNF-$\alpha^{-/-}$ mice were treated with TLR-L (1 μg/ml LPS plus 100 ng/ml P3C) for 24 h, and levels of IL-10, IL-12 p40, and TNF-α in the culture supernatants were determined by ELISA (Fig. 1A). Consistent with our previous study, TLR-L induced substantial level of IL-10 production by WT DCs. Notably, IL-10 production by TNF-$\alpha^{-/-}$ DCs stimulated with TLR-L was significantly suppressed as compared to that by WT DCs (Fig. 1A, left). In contrast, both WT DCs and TNF-$\alpha^{-/-}$ DCs vigorously produced IL-12 p40 in response to TLR-L and no significant difference was detected in this cytokine production between these types of DCs (Fig. 1A, center). WT DCs markedly produced TNF-α in response to TLR-L, while TNF-$\alpha^{-/-}$ DCs showed no TNF-α production irrespective of the TLR stimulation (Fig. 1A, right). We also analyzed IL-12 p70 production by WT and TNF-$\alpha^{-/-}$ DCs upon TLR stimulation. However, no IL-12 p70 production was detected in any cultures tested (<30 pg/ml, data not shown). No significant difference was detected in the cell viability between WT and TNF-$\alpha^{-/-}$ DCs after 24 h of culture (data not shown).

3.2. The effect of exogenous TNF-α in IL-10 production by DCs upon TLR stimulation

Above findings (Fig. 1A) suggest that DC production of TNF-α lead to the IL-10 production by these DCs in response to TLR ligands. We next examined whether addition of exogenous TNF-α during the TLR stimulation recovered the impaired ability of TNF-$\alpha^{-/-}$ DCs to produce IL-10.

BMDCs from WT or TNF-$\alpha^{-/-}$ mice were stimulated with TLR-L in the presence or absence of TNF-α 100 ng/ml for 24 h, and levels of IL-10 and IL-12 p40 in the culture supernatants were determined by ELISA (Fig. 1B). TNF-α alone never induced IL-10 production by both types of DCs (Fig. 1B left). Again, TLR-L induced vigorous production of IL-10 by WT DCs but not by TNF-$\alpha^{-/-}$ DCs. Addition of TNF-α restored the TLR-mediated IL-10 production by TNF-$\alpha^{-/-}$ DCs to the level of that by WT DCs. In contrast, TNF-α showed no significant effect on TLR-L mediated IL-10 production by WT DCs. Thus, TNF-α produced by WT DCs may be necessary to induce maximal IL-10 production by the DCs in response to TLR-L.

TLR-L markedly induced IL-12 p40 production by WT DCs and TNF-$\alpha^{-/-}$ DCs, and no significant difference was detected in the level of IL-12 p40 production between these types of DCs (Fig. 1B, middle). Exogenous TNF-α never affected the TLR-mediated IL-12 p40 production by WT DCs. Although TNF-α slightly increased the TLR-mediated IL-12 p40 production by TNF-$\alpha^{-/-}$ DCs, the effect was statistically not significant.

3.3. Cell surface expressions of maturation markers on TLR-stimulated DCs

We next analyzed the cell surface expression of several maturation markers on WT and TNF-$\alpha^{-/-}$ DCs. WT and TNF-$\alpha^{-/-}$ DCs were treated with TLR-L for 24 h and the cell surface expressions of CD40, CD86, and I-A^b were determined by flow cytometry (Fig. 2). After the TLR stimulation, WT and TNF-$\alpha^{-/-}$ DCs exhibited mature phenotype, high expression of CD86, CD40, and I-A^b. No significant difference was detected in the expression level of these maturation markers between WT and TNF-$\alpha^{-/-}$ DCs, although the proportion of CD86 positive cells was increased in TNF-$\alpha^{-/-}$ DCs compared to WT DCs (Fig. 2). Addition of TNF-α during the TLR stimulation showed no effect on the level of CD86, CD40, and I-A^b expressions in both types of DCs (data not shown). From these results, TNF-α may be dispensable for the phenotypic maturation of DCs in response to TLR stimulation.

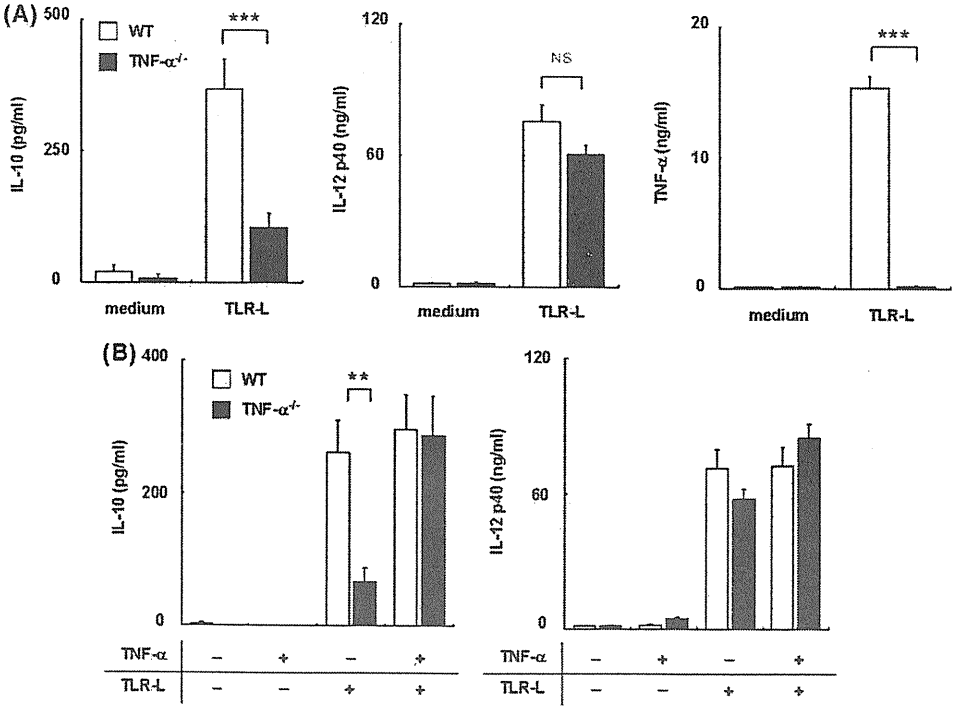

Fig. 1. Cytokine production by WT and TNF-$\alpha^{-/-}$ DCs upon TLR stimulation. (A) BMDCs from WT or TNF-$\alpha^{-/-}$ mice were stimulated with 1 μg/ml LPS plus 100 ng/ml P3C (TLR-L) for 24 h. (B) BMDCs from WT or TNF-$\alpha^{-/-}$ mice were stimulated with TLR-L in the presence or absence of TNF-α (100 ng/ml) for 24 h. The amount of cytokines in the culture supernatants was measured by ELISA. Each column represents the mean ± SE of 11 (A) or nine (B) independent experiments. Statistical significance was calculated by Student's *t*-test (**$p < 0.01$; ***$p < 0.001$; NS, not significant).

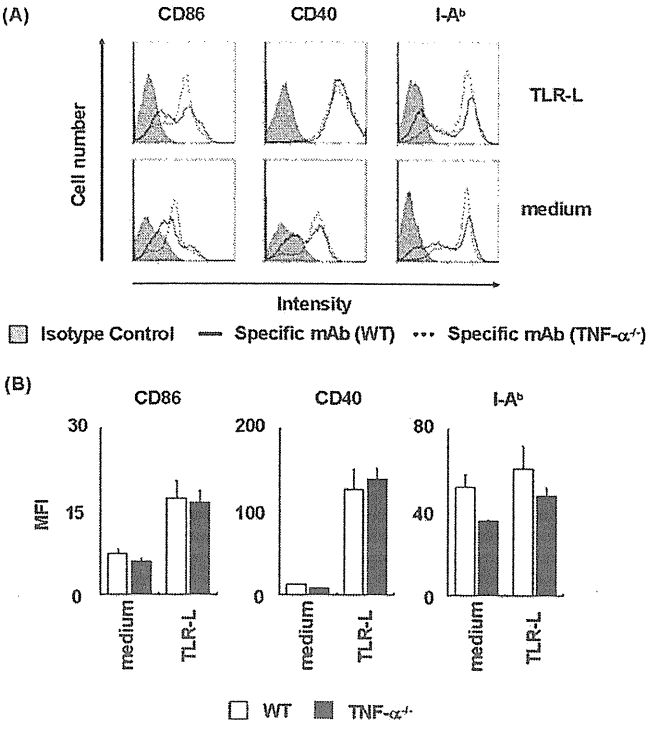

Fig. 2. Expression of surface molecules on WT and TNF-$\alpha^{-/-}$ DCs upon TLR stimulation. BMDCs from WT or TNF-$\alpha^{-/-}$ mice were stimulated with TLR-L for 24 h. Expressions of CD86, CD40, and I-A^b were analyzed by flow cytometry. (A) Representative histogram of the each molecule on WT and TNF-$\alpha^{-/-}$ DCs. (B) Each column represents the mean ± SE of three independent experiments. MFI, mean fluorescence intensity.

3.4. The effect of TNF-α on activation of Akt and MAPKs in DCs upon TLR stimulation

PI3K/Akt and MAPK pathways are responsible for production of various cytokines following TLR stimulation [36]. It has been reported that TNF-α is capable of activating these intracellular pathways [37,38]. TNF-α promoted IL-10 production in TNF-$\alpha^{-/-}$ DCs but not in WT DCs (Fig. 1). To analyze the molecular mechanism responsible for the TNF-α-mediated promotion of IL-10 production seen in TNF-$\alpha^{-/-}$ DCs, we examined the effect of TNF-α on activation of Akt and MAPKs (ERK1/2, p38 MAPK, and JNK1/2) in the TNF-$\alpha^{-/-}$ DCs upon TLR stimulation.

BMDCs from TNF-$\alpha^{-/-}$ mice were stimulated with TNF-α and/or TLR-L for indicated time periods, and intracellular protein levels of phospho-Akt (pAkt), phospho-ERK1/2 (pERK1/2), phospho-p38 MAPK (pp38 MAPK), and phospho-JNK1/2 (pJNK1/2) were determined by immunoblotting (Fig. 3).

TNF-α markedly increased the level of pERK1/2 in TNF-$\alpha^{-/-}$ DCs at 7 min, while showed only slight effect at 15–30 min (Fig. 3A and B). On the other hand, TLR-L induced slight phosphorylation of ERK1/2 in TNF-$\alpha^{-/-}$ DCs at 7 min, but markedly increased the level at 15 min. The effect was decreased at 30 min. The pERK1/2 in TNF-$\alpha^{-/-}$ DCs at 7 min after treatment with both TLR-L and TNF-α showed same level as that in TNF-$\alpha^{-/-}$ DCs treated with TNF-α alone. Thus, the ERK1/2 activation at 7 min seemed to be largely dependent on TNF-α. At 15 and 30 min no difference was detected in the pERK1/2 level between TLR-L-treated and TLR-L plus TNF-α-treated TNF-$\alpha^{-/-}$ DCs.

The levels of pp38 MAPK and pAkt in TNF-$\alpha^{-/-}$ DCs were markedly increased at 7 min, and then gradually reduced at 15–30 min after TNF-α stimulation (Fig. 3A, C, and E). In contrast, TLR-L increased the levels of these molecules slightly at 7 min, but markedly at 15 and 30 min. Treatment of these DCs with both TNF-α and TLR-L considerably increased the levels of pp38 MAPK and pAkt at 7 min as compared with those in DCs treated with TLR-L alone. Thus, exogenous TNF-α was responsible for an early (7 min) activation of p38 MAPK and Akt.

The level of pJNK1/2 in TNF-$\alpha^{-/-}$ DCs was modestly increased at 7 to 15 min and then decreased at 30 min after TNF-α stimulation (Fig. 3A and D). In contrast, TLR-L increased the level of pJNK1/2 modestly at 7 min and markedly at 15 and 30 min. Exogenous TNF-α, however, showed no significant effect on the TLR-L-mediated phosphorylation of pJNK1/2 at all time periods tested.

3.5. The effect of ERK1/2, p38 MAPK, or PI3K inhibition on IL-10 and IL-12 p40 production by TNF-$\alpha^{-/-}$ DCs upon TNF-α plus TLR-L stimulation

ERK1/2, p38 MAPK, and Akt activation in TNF-$\alpha^{-/-}$ DCs upon TLR stimulation was significantly enhanced by addition of TNF-α at an early time point (Fig. 3). We thus examined the role of ERK1/2, p38 MAPK, and Akt in IL-10 production by TNF-$\alpha^{-/-}$ DCs upon stimulation with TLR-L plus TNF-α using U0126, a specific inhibitor of MEK-ERK pathway, SB203580, a specific inhibitor of p38 MAPK, and LY294002, a specific inhibitor of PI3K.

TNF-$\alpha^{-/-}$ DCs were pretreated with U0126, SB203530, LY294002, or vehicle alone (0.1% DMSO) for 1 h and then stimulated with TNF-α and/or TLR-L for 24 h in the presence of each inhibitor. The amount of IL-10 and IL-12 p40 in the culture supernatant was quantitated by ELISA (Fig. 4). Again, stimulation with TLR-L plus TNF-α induced vigorous production of IL-10 and IL-12 p40. U0126 modestly inhibited the IL-10 production and increased the IL-12 p40 production by TNF-$\alpha^{-/-}$ DCs. Notably, both SB203580 and LY294002 markedly inhibited the IL-10 production by TNF-$\alpha^{-/-}$ DCs upon TLR-L plus TNF-α stimulation, while showing no significant effect on the IL-12 p40 production. Thus, the TNF-α-mediated early activation of ERK1/2, p38 MAPK, and PI3K/Akt may be responsible for the promotion of IL-10 production by TNF-$\alpha^{-/-}$ DCs upon TLR stimulation.

4. Discussion

TLR ligands induce vigorous production of pro-inflammatory cytokines by macrophages and DCs. These TLR-mediated innate immune responses are crucial to initiates acquired immunity. TLR ligands also induce production of IL-10, an anti-inflammatory cytokine, which may suppress undesirable and/or exceeded inflammatory responses. Although transcription factors and signal transduction pathways for production of pro-inflammatory cytokines have been well identified, those of anti-inflammatory cytokines such as IL-10 have been elusive. In the present study, we examined the role of TNF-α in DC production of IL-10 upon TLR4 and TLR2 stimulation (TLR4,2 stimulation) and pursued mechanism underlying the TNF-α-mediated regulation of IL-10 production. We demonstrated herein that TNF-α was involved in DC production of IL-10 but not IL-12 p40 upon TLR4,2 stimulation. It was also shown that the TNF-α-mediated activation of MAPK and PI3K/Akt pathways may be responsible for the TNF-α-mediated regulation of IL-10 production.

First, we compared productions of IL-10 and IL-12 p40 between WT and TNF-$\alpha^{-/-}$ DCs in response to TLR-L (LPS plus P3C). Upon TLR4,2 stimulation, TNF-$\alpha^{-/-}$ DCs produced lower level of IL-10 than those by WT DCs. In contrast, no significant differences were noted in the TLR-mediated IL-12 p40 production between these types of DCs. Addition of TNF-α during the TLR stimulation recovered the impaired ability of TNF-$\alpha^{-/-}$ DCs for IL-10 production, although TNF-α alone exerted negligible effect on the IL-10

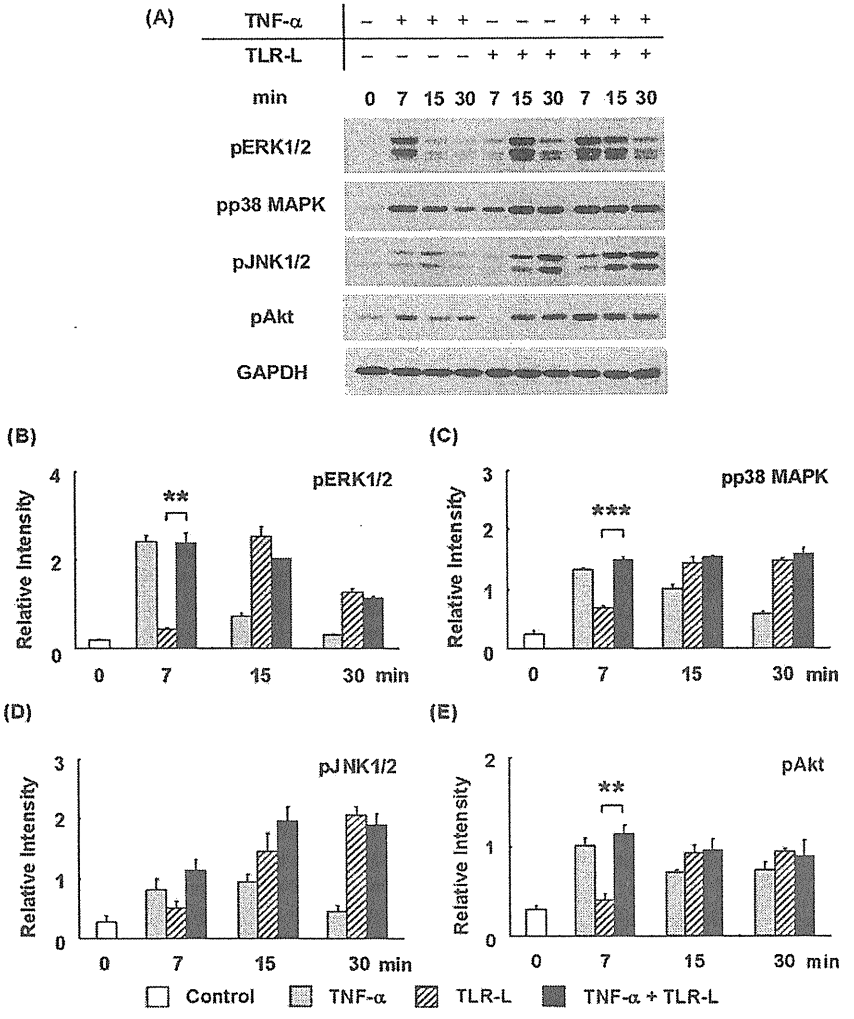

Fig. 3. Activation of ERK1/2, p38 MAPK, JNK1/2, and Akt in TNF-$\alpha^{-/-}$ DCs upon stimulation with TNF-α and TLR-L. BMDCs were treated with TNF-α (100 ng/ml) and/or TLR-L for 7, 15, or 30 min, and whole cell lysates were prepared. Levels of phospho-ERK1/2 (pERK1/2), phospho-p38 MAPK (pp38 MAPK), phospho-JNK1/2 (pJNK1/2), and phospho-Akt (pAkt) in the cell lysates were determined by immunoblotting. GAPDH level was determined as an internal control for each sample. (A) Representative immunoblot is shown. (B) The relative intensity of the specific band is shown. Each column represents the mean ± SE of three independent experiments. Statistical significance was calculated by Student's *t*-test (**$p < 0.01$; ***$p < 0.001$).

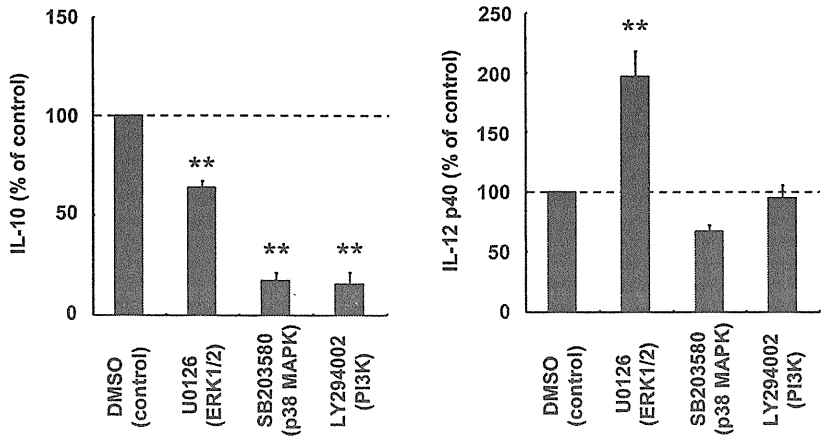

Fig. 4. The effect of ERK1/2, p38 MAPK, or PI3K inhibition on IL-10 and IL-12 production by TNF-$\alpha^{-/-}$ DCs stimulated with TNF-α plus TLR-L. BMDCs were pretreated with 10 μM U0126 (a MEK1/2 inhibitor), 30 μM SB203530 (a p38 MAPK inhibitor), 10 μM LY294002 (a PI3K inhibitor), or vehicle alone (0.1% DMSO) for 1 h and then stimulated with TNF-α (100 ng/ml) plus TLR-L for 24 h in the presence of each inhibitor. The amount of IL-10 and IL-12 in the culture supernatants was measured by ELISA. Each column represents the mean ± SE of five independent experiments. Statistical significance was calculated by Dunnett's test (**$p < 0.01$).

production. It seems that TNF-α is involved in the enhancement of TLR-mediated production of IL-10, while this cytokine-mediated signaling alone is insufficient to induce a substantial level of IL-10 production by DCs.